universität wien

MASTERARBEIT / MASTER'S THESIS

Titel der Masterarbeit / Title of the Master's Thesis

Pyrazoloquinolinones: To bind or not to bind - the GABAA receptor trans membrane domain (TMD).

verfasst von / submitted by

Benjamin Schaar, BSc

angestrebter akademischer Grad / in partial fulfilment of the requirements for the degree of

Master of Science (MSc)

Wien, 2021 / Vienna, 2021

Studienkennzahl lt. Studienblatt / degree programme code as it appears on the student record sheet:	**UA 066 834**
Studienrichtung lt. Studienblatt / degree programme as it appears on the student record sheet:	**Masterstudium Molekulare Biologie**
Betreut von / Supervisor:	**Dr. Margot Ernst, Priv. Doz.**

Table of contents

List of figures

List of tables

Abstract

Pyrazoloquinolinones (PQs) are promising compounds for $GABA_A$ receptor subtype selective drugs. There is a lot of data showing that many PQ derivatives bind at a novel site at the extra cellular domain (ECD α+/β- interface), where they exert positive allosteric modulation (PAM). So far, no compound has been identified that exclusively binds to the ECD α+/β- interface. Compounds binding exclusively to the ECD α+/β- interface activate different receptor pools than compounds acting on the canonical benzodiazepine binding site and thereby might have different in vivo effects. Many PQs are also binding the β+/α- interface in the trans-membrane domain (TMD) but for many derivatives there is no data about the involvement the TMD available. The involvement of more than one binding site in the efficacy of PQs is a drawback in terms of finding a receptor subtype selective PQ, especially because amino acids in the TMD interfaces are better conserved across different receptor subtypes. Therefore, gathering data about the involvement of the TMD interface in the efficacy of PQs becomes necessary to better understand which ligand features promote binding/ non-binding. In this work, the efficacy of seven PQ derivatives (PZII-028, DCBS120, DCBS199, DCBSPU51, DCBSPU53, LAU176, LAU177) was measured with two-electrode voltage-clamp (TEV) electrophysiology in α1β3, α1β3N265S, α1β3N41R and α1β1 receptors. While some of the compounds (LAU176, LAU177, DCBSPU53, DCBS120) seem to bind at the TMD interface, one compound (DCBS199) shows selectivity for the ECD α+/β- interface in α1β1 receptors without binding at the TMD interface. A ligand feature which promotes binding to the TMD β+/α- interface in α1β3 receptors seems to be a hydrogen bond acceptor in position R'4. Additionally, compounds with a hydrogen bond acceptor on position R'4 show higher efficacy in α1β3 wildtype receptors. One compound (DCBS120) seems to bind the β+/α- interface in α1β1 wildtype receptors and is substituted with a hydrogen bond donor at position R'3. Two compounds (DCBS120, DCBS199) show higher efficacy in α1β1 wildtype and both have amino substituents on ring D at either position R'3 (DCBS120) or R'4 (DCBS199). The subtype preference and TMD binding behaviour of the PQs in this work tends to be influenced by ring D substitutions, while ring A substitutions tends to have no influence. Lastly a virtual screening was performed with Ligand Scout to screen a library of 57 PQs, of which some were predicted to also bind the TMD β+/α- interface. The total body of data leads to improved compound design.

Chapter 1: Introduction

The $GABA_A$ receptors, as one of the most complex ligand gated ion channel families in terms of receptor subtypes and protein-ligand interaction possibilities (Johnston, 1996; Olsen & Sieghart, 2009), still leave open questions regarding many known ligands and their pharmacological profile (Sieghart & Savic, 2018). The complexity of these hetero pentameric proteins arises due to a high number of variable subunits which can incorporate into the receptor. The known mammalian subunit isoforms are: α(1–6), β(1–3), γ(1–3), δ, ε, θ, π and ρ(1–3) (Wongsamitkul et al., 2017). Depending on the incorporated subunits, many different receptor subtypes and binding interfaces for ligands can theoretically form and vary in their pharmacological properties (Sarto-Jackson & Sieghart, 2008). While many subtypes can form in vitro, only a few have been observed to form in vivo (Johnston, 1996; Olsen & Sieghart, 2009).

One group of those described ligands are pyrazoloquinolinones (abbreviated as "PQs"). The prototypical PQ, named CGS8216, was discovered years ago and based on that scaffold many variations with different substituents at certain positions where synthesized. The different substituents create a high variety of possible ligand-protein interactions and can even induce stereochemical differences between ligands (Treven et al., 2018), which makes them a perfect toolbox for unlocking receptor subtype selective binding and rational drug design (Simeone et al., 2017).

In 2011 a novel binding site has been described in the extra cellular domain at the (ECD) α+/β- Interface, which made PQ's promising drugs for selective $GABA_A$ modulation (Ramerstorfer et al., 2011), but there are some issues to be considered. On the one hand, many of the PQs may bind to additional binding sites like the interfaces in the trans membrane domain (TMD) (Iorio et al., 2019; Maldifassi et al., 2016) which compromises their ability to be receptor subtype selective binders at the ECD α+/β- interface. Another issue is the recently hypothesized differences in binding modes (Fabjan et al., 2021), which make it hard to apply structure-function relationships between closely related PQ molecules and thereby makes it very difficult to rationally design variants of these ligands. However, many variants were synthesized and most of them are still missing experimental data to clarify their full pharmacological profile, therefore their real potential remains an open question.

1.1 Ligands and their Effects on $GABA_A$ Receptors

Like other receptors, $GABA_A$ receptors can bind small molecules and ligands at certain binding

sites and these ligand-protein interactions subsequently induce changes in structure and function of the protein. Since $GABA_A$ receptors are anion channels changes in function manifest in a change in chloride ion or bicarbonate influx (Olsen, 2015).

The three existing types of orthosteric ligands are agonists, antagonists, and inverse agonists. The agonistic effects are similar to effects generated by the endogenous ligand GABA which upon binding induces ion influx. The counterpart to agonists are antagonists which often compete for the agonistic binding site and thereby counteracting the strength of receptor activation. Lastly there are inverse agonists which not only counteract the effect induced by agonists but also being able to induce an opposite effect (Vega Alanis et al., 2020).

In addition to the orthosteric ligands there are also allosteric ligands. Among the best-known are positive allosteric modulators (PAM) such as diazepines. PAMs will only enhance ion currents if an agonist is already bound. Some PAMs like ligands of the canonical benzodiazepine binding site won't even modulate beyond $GABA_A$ max currents. This behaviour is favourable since overdosing with this type of ligands is barely possible. Besides there are also negative- and silent- allosteric modulators. Flumazenil, for example, which is used as an antidote to benzodiazepine intoxication or anaesthetics, binds to the allosteric binding site and acts as a silent allosteric modulator (SAM) which means it competes for the same binding site without effecting ion influx. When a negative allosteric modulator(NAM) like Ro15-4513 binds it shows the opposite effects compared to PAMs and it is decreasing chloride ion influx induced by agonists (Olsen, 2015; Vega Alanis et al., 2020).

Binding of ligands at one binding site can also affect ligands at other binding sites via allosteric crosstalk. One example is the effect of picrotoxin. When it binds to its binding site in the TMD it behaves like a competitive inhibitor for the agonist GABA at the agonistic binding site in the ECD. Normally a competitive inhibitor would compete for the same binding site, but in this case the effect is transduced via allosteric cross-talk between two different binding sites (Masiulis et al., 2019).

1.2 Pyrazoloquinolinones

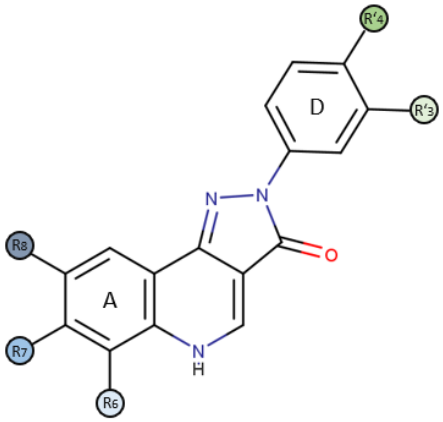

Figure 2 - PQ Scaffold - 2-phenyl-2H-pyrazolo[4,3-c]quinolin-3(5H)-one and marked positions of varying substituents.

Since their early appearance in $GABA_A$ research in the 1980's (Mohler et al., 1982) a lot of variations regarding their substitutions at different positions have been synthesized but only for some of them functional data exists (Fabjan et al., 2021; Simeone et al., 2019; Simeone et al., 2017; Treven et al., 2018; Varagic et al., 2013). The PQ's which are focus of this work are built on the scaffold of 2-phenyl-2H-pyrazolo[4,3-c]quinolin-3(5H)-one (**Figure 1)** and the marked substituent positions are the atoms that can differ between the PQ derivates. The substituents are either located on ring A or ring D. This gives rise to a lot of different binding site interaction possibilities. Additionally, the single bond between ring C and ring D allows the molecule to

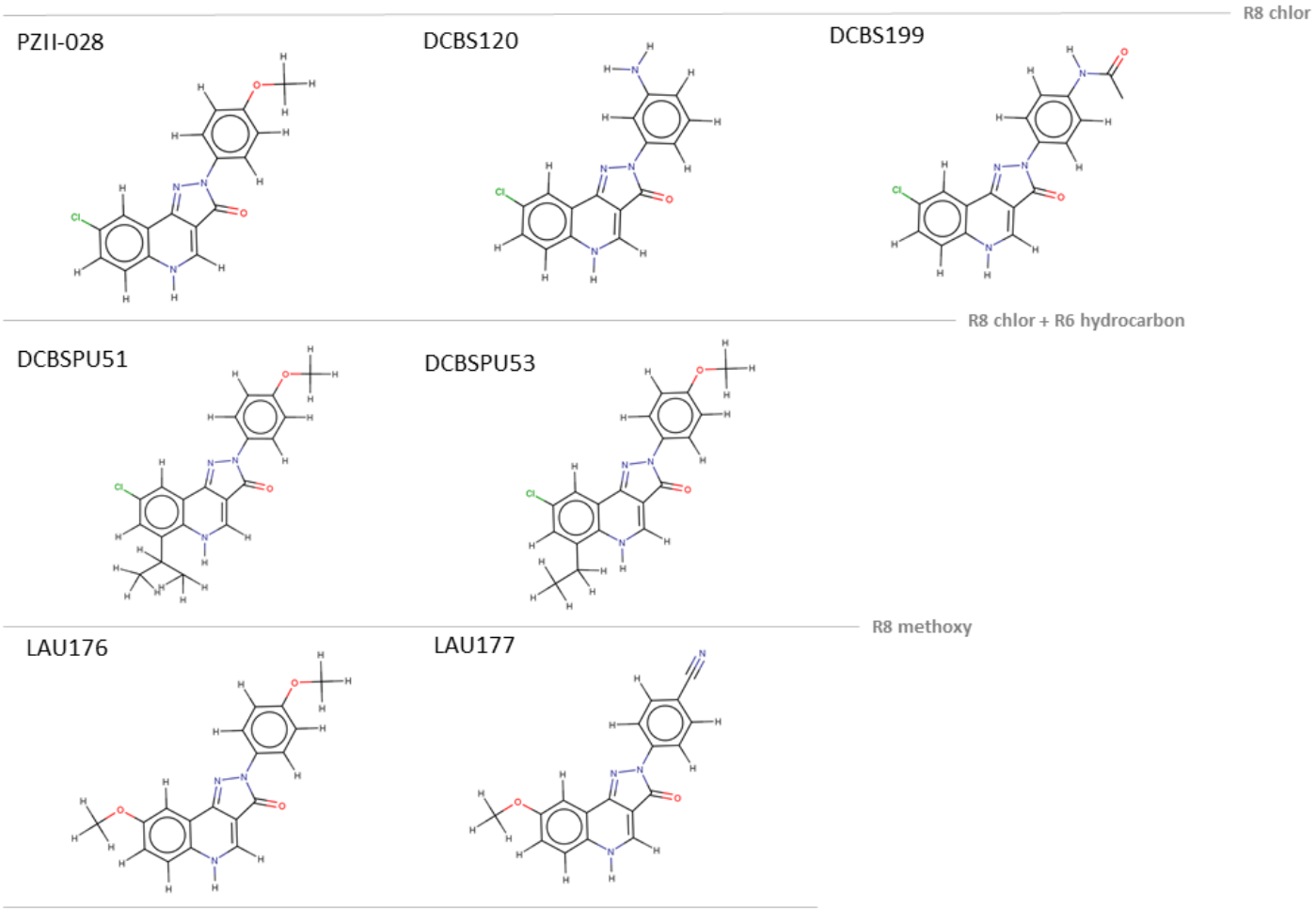

Figure 1 - PQ-types analysed in this work: **DCBS120** (R8=Cl, R'3=NH_4), **LAU176** (R8=OMe, R'4=OMe), **LAU177** (R8=OMe,R'4=CN), **PZII-028** (R8=Cl,R'4=OMe), **DCBSPU51** (R8=Cl, R6=iPr, R'4=OMe), **DCBSPU53** (R8=Cl, R6=Et,R'4=OMe), **DCBS199** (R8=Cl,R'4=NHAc)

interact with binding sites by rotating and adapting depending on the environment in the binding site and the substituent types of the PQ (Treven et al., 2018; Varagic et al., 2013).

As a result of this very heterogeneous compound class that can bind and modulate $GABA_A$ receptors, efforts have been made to investigate the structure-function relationship of various substituents and substituent combinations especially regarding $GABA_A$ subtype selectivity (Nilsson et al., 2011; Shindo et al., 1989; Simeone et al., 2017; Treven et al., 2018).

In 2017 the first subtype selective PQs being selective for β1 containing receptors were found (Xenia Simeone et al., 2017). Soon after also PQs being selective for α6β(2-3)γ2 were found (Treven et al., 2018).

Nevertheless, it remains a challenge to predict functional selectivity from ligand features. PQs with substituents in position R8 and R'3 seem to have lower efficacy but higher functional selectivity. Adding large substituents like tert-butyl on position R8 reduces affinity for the ECD α+/ γ- Interface. Limited β selectivity can be induced by adding substituents in position R8 and R'4 (Fabjan et al., 2021).

Figure 2 shows the PQ derivates that were analysed in this work with different substitutions. For some of them (**LAU176, LAU177, PZII-028**) efficacy data is already available and summarized in a study by Fabjan et al. (2021).

1.3 PQ-Binding Sites

In the first instance, the PQs' ability to bind to the canonical benzodiazepine binding sites at the ECD α+/γ- Interface was identified and depending on the PQ type, induces different effects via this binding site. While CGS8216 was hypothesized to be a weak inverse agonist, meaning that it reverses the effects of diazepam and sometimes has minor opposite effects, CGS9896 showed attributes of a mixed agonist/antagonist (Boast et al., 1985). Later, Ramersdorfer et al. (2011) clarified the precise effects of CGS9895 by a steric hindrance approach. He concluded that the ligand is acting as a high affinity antagonist at the ECD α+/ γ- Interface in most receptor subtypes but approaching micromolar ligand concentrations also start enhancing GABA mediated currents at least partly via the ECD α+/β- Interface (**Figure 3**). Interestingly the effect generated by the nanomolar ECD α+/ γ- Interface seems to be receptor subtype dependent, since in α3β3γ2 receptors the compound is also acting as a weak positive allosteric modulator via this high affinity site explaining the benzodiazepine like in vivo effects from that compound at physiological

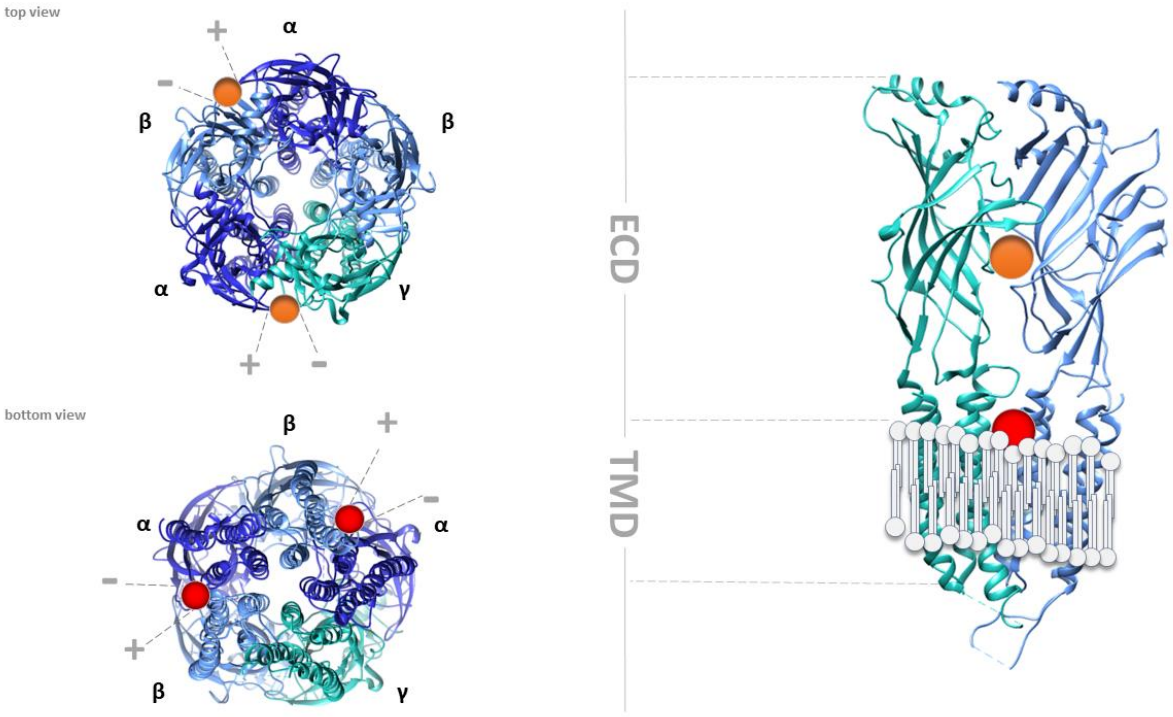

Figure 3 | Representation of stereotypical GabaA Rezeptor. Orange cycles indicate ECD binding Interfaces for PQs (α+/γ- Interace, α+/β- Interface). Red cycles indicate the TMD Interfaces at the β +/ α- Interface. In the sideview the orange dots indicate the vertical position of both homologous types of ECD Interfaces (Note that it is only scematic since both interfaces wouldn't be stacked in the sideview).

concentrations in the nanomolar range (Ramerstorfer et al., 2011).

Via a computational approach Fabjan et al. (2021) hypothesized that most PQs can bind the ECD α+/β- Interface (**Figure 3**). Strong modulating PQs such as LAU177 seem to generate their effect not only via the more interesting ECD α+/β- Interface, the TMD β+/α- Interface also contributes to a large extent. This makes it harder to find receptor subtype selective PQs since the TMD Interfaces are very conserved in many $GABA_A$ receptor subtypes (Fabjan et al., 2021). This means that a subtype selective PQ binding to the ECD α+/β- Interface might also bind unselectively to other receptor subtypes at the TMD β+/α- Interface and the subtype selective effect is abolished.

This involvement of the TMD β+/α- Interface is also in line with Ramersdorfer et al. (2011) mutational analysis. He showed a reduced efficacy for CGS9895 and LAU177 by inducing the N265I mutation into the β2 subunit of his receptors (Ramerstorfer et al., 2011).

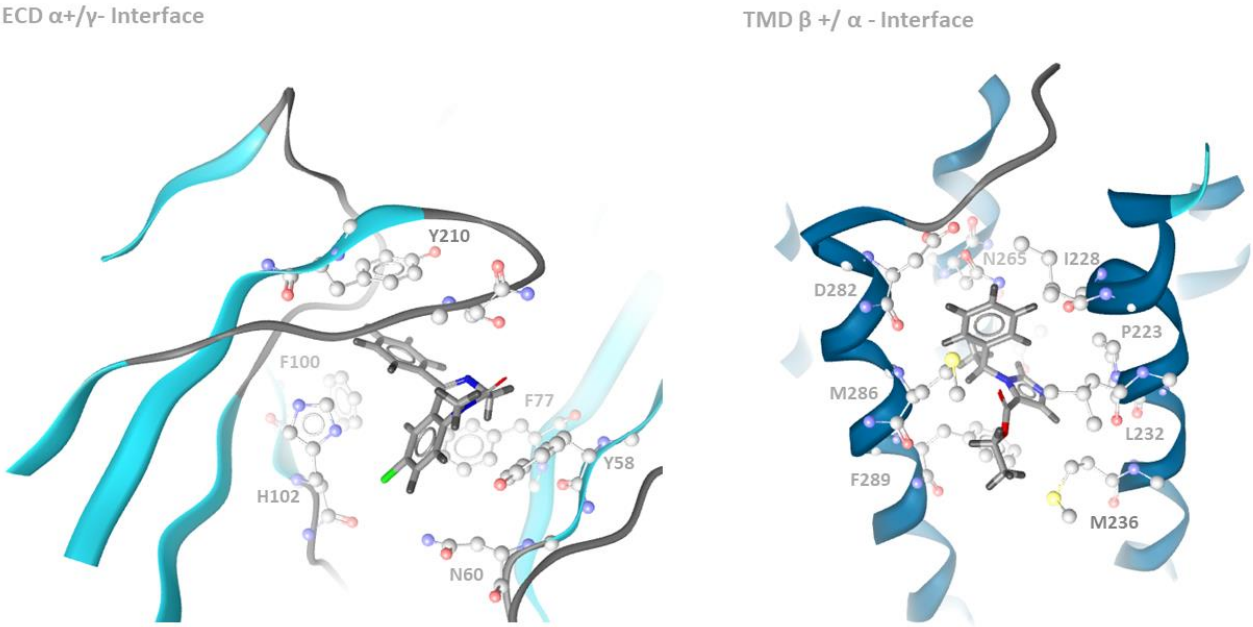

Figure 4 | Detailed view of the ECD α+/γ- Interace and the TMD β +/ α- Interface with bound diazepam. PDB ID: 6HUP (Masiulis et al., 2019). Named amino acids are important for ligand effects in the associated binding site.

1.3.1 ECD α+/γ- Interface

The ECD α+/γ- Interface is widely known as the canonical benzodiazepine binding site. Well known compounds such as diazepam and alprazolam exert some of their effects via this site. **Figure 4** shows a representation of this interface with diazepam in the bound state (Masiulis et al., 2019).

At this site most PQs bind at nanomolar concentrations and act as antagonist or weak PAM which makes this site less interesting for strong subtype selective PQ effects (Carotti et al., 2003; Fabjan et al., 2021; Knutson et al., 2018).

1.3.2 ECD α+/β- Interface

Since Ramersdorfer et al. (2011) discovered that PQs also act via the ECD α+/β- Interface at micromolar concentrations, a lot of PQ variants were also confirmed to exert their effects partly via this site (Fabjan et al., 2021).

The fact that the ECD α+/β- Interface also exists in receptors not containing the γ-subunit gives compounds acting on that interface additional target receptors not used by compounds which bind to the canonical benzodiazepine binding site (Olsen & Sieghart, 2009).

Until this day no ligand is known which exclusively binds to this interface and therefore it remains unknown if and how a drugs effect acting only via this site would differ to other drugs acting exclusively on other interfaces and efforts are being made to find such compounds of interest (Iorio et al., 2020).

1.3.3 TMD β +/ α- Interface

There is strong evidence suggesting that the TMD β+/α- Interface is the site of action of general anaesthetics such as etomidate or propofol. The anaesthetic effect of diazepam at higher concentrations also seems to be generated by binding of diazepam to this site, where it binds with much lower affinity in relation to its classical ECD binding site (Kim et al., 2020).

The anaesthetics effect induced by ligands acting on $GABA_A$ receptors was recently hypothesized to be dependent on the general stabilisation of the TMD domain via binding of ligands at these interfaces and thereby pulling the TMD domain closer together. Considering this also the antagonistic effect of flumazenil to reverse anaesthesia was proposed to be induced not only by local interactions at its site of action at the ECD γ+/β- Interface, but also by allosteric effects induced to the TMD β+/α- Interface, making it impossible for diazepam or etomidate to bind there and therefore counteracting their ability to act on this site (Kim et al., 2020).

An important amino acid that was shown to induce the TMD stabilising effect of compounds such as diazepam, etomidate and PQs seem to be the amino acid asparagine 265 of β2/β3. Additionally also mutations to the methionine at position 236 in β3 induce a total loss of efficacy of etomidate and propofol. (Kim et al., 2020; Maldifassi et al., 2016)

For many PQs a lot of experimental data is already available, especially regarding their usage of the ECD α+/β- Interface and the ECD α+/γ- Interface. What is missing is experimental data regarding the TMD interfaces. Therefore, the aim of this work is to focus on the TMD β+/α- Interface, known to convey the anaesthetic effect of many clinically used compounds. With enough experimental data it might one day become possible to rationally design PQs with substituents and substitutional patterns that generate specific binding site usage and receptor subtype selectivity and do not use TMD sites.

1.4 The prospect of subtype selective ligands

Looking at the expression of the different subunits in the brain which form the $GABA_A$ receptors, we find that some subunits are expressed ubiquitously throughout the brain and others are only expressed locally in certain cell types and brain regions. Rather generally expressed subunits are α1, β1, β2, β3, and γ2. Localized expression is especially strong for the α6 subunit being highly expressed in the cerebellum. The α4 subunit is also quite narrowly expressed in the thalamus, hippocampus, olfactory tubercle, and basal ganglia (Laurie et al., 1992; Nutt, 2006; Pirker et al., 2000). This might lead to the hypothesis that by modulating certain receptor subtypes localized in certain brain regions with receptor subtype selective ligands, one might induce a narrower scope pf pharmacological effects generated by these ensembles of receptors.

It was shown in mice by inducing a point mutation that renders a certain α subunit benzodiazepine insensitive that specific subtypes of receptors seem to generate specific effects such as α1 containing receptors inducing the sedative effects of benzodiazepines but to a lesser extent the anxiolytic effects and α2 containing receptors being more responsible for the anxiolytic effects (Olsen, 2015).

Additionally, it was observed that also the γ2 subunit contributes to the anxiolytic effect of benzodiazepines. Mice with reduced γ2 expression due to a genetic knockout had reduced anxiolytic response to benzodiazepines but similar hypnotic response (Nutt, 2006). On the other hand it seems logic that if one reduces the expression of the γ2 subunit, as the most expressed γ-type subunit in mouse brain (Hörtnagl et al., 2013), some of the effects induced by benzodiazepines via the α+/ γ- Interface will be shifted.

Since brain regions are not locally isolated but interconnected, recent findings also highlight the involvement of changes in network dynamics regarding the anxiolytic effect of benzodiazepines. It was shown that the anxiolytic effect is not only generated by binding and general downregulation of neurons in the central amygdala but also by a shift in network dynamics in the central amygdala. Benzodiazepine sensitive, meaning α2 and γ2 expressing, SST+/PKCδ- neurons show decreased activity and thereby PKCδ+/SST- neurons, which are under inhibitory control by SST+/PKCδ- neurons increase their activity which ultimately leads to decreased central medial amygdala output trough inhibitory gating induced by activated PKCδ+/SST- neurons and subsequently a reduced fear response (Griessner et al., 2021).

Taken together these previous findings illustrate the potential benefits of α2 selective ligands for

the anxiolytic effect but what might ligand selective for other subtypes do? To unlock these unknowns, one might need a diverse set of potential "keys" like the diversely substituted pyrazoloquinolinones.

1.5 Mutational studies and rationale of used mutations

To analyse the involvement of a binding site in the pharmacology of a certain ligand, conversion mutations of amino acids important for ligand-protein interactions can be used which may lead to a partial or total loss of efficacy. To find important amino acids for ligand-protein contact, structures from the protein data base (PDB) and their respective publications can be used where a lot of information can be extracted regarding amino acids and their interactions with ligand features (Kim et al., 2020; Stewart et al., 2014).

In many cases certain point mutations can completely disrupt the effect of ligands. A well-known example is the α H101 residue inside the ECD α+/γ- Interface. When it is mutated to R like it is in the benzodiazepine insensitive α4 and α6 subtypes, positive allosteric modulation by benzodiazepines is abolished (Olsen, 2015).

Another example is the amino acid β N265 inside the TMD β +/ α- Interface. It was shown that mutating this amino acid to M or C greatly decreases efficacy of the anaesthetics etomidate and propofol (Stewart et al., 2014). The PQs CGS9895 and LAU177 as well as diazepam were shown to loose efficacy when the β N265 amino acid was muted to I (Maldifassi et al., 2016).

For this work α1β3 wildtype receptors were mutated either at the ECD α+/β- Interface or at the TMD β+/ α- Interface. For both interfaces a conversion mutation, which converts an amino acid of the respective binding site into the homologous amino acid in the α1β1 wildtype was used.

The mutation used in the ECD α+/β- Interface was the β3 N41R mutation. The efficacy of the PQs were then measured in α1β3 and α1β1 wildtype to compare weather a conversion mutation at β3 subunit changes the efficacy to a similar value as seen in the α1β1 wildtype and thereby conclusions about binding site usage can be made (Simeone et al., 2017).

A similar approach was used for the TMD β +/ α- Interface where the β3 N265S mutation was used. It is again a β3 to β1 conversion mutation regarding the single amino acid because β1 containing receptors were shown to be less sensitive to anaesthetics like etomidate (Hill-Venning et al., 1997). Besides, β3 N265 is important for efficacy at that binding interface in general.

1.6 Virtual Screening Tools - Ligand Scout

Virtual screening methods can be a valuable computational toolbox for searching large libraries of ligands and identifying candidates that might interact with a certain binding site of choice. Old concepts such as pharmacophore models combined with increasingly available structural data are currently regaining popularity and generating valuable data for low cost (Sanders et al., 2012).

A 3D-pharmacophore can describe a molecule by 3-dimensionaly arranged molecular features that can interact with a binding site. There are structure-based and ligand-based pharmacophore models. Structure based pharmacophore models reduce the number of features depending on the environment in the binding site and therefore they need ligand-protein complexes deposited in the Protein Data Base. Ligand-based pharmacophore models are generated by all possible interacting features of the ligand and are used when no data of ligand-protein complexes is available (Wolber & Langer, 2005, Ligand Scout Manual).

Ligand Scout can create structure- and ligand-based 3D-pharmacophore models and these models can then be used for screening virtual databases of ligands. Additionally, Ligand Scout offers the possibilities to dock ligands into a binding site and subsequently rank docking poses based on various scoring functions and create pharmacophore models from selected poses. A comparative analysis of various virtual screening tools concluded that overlay based methods such as Ligand Scout deliver a better true positive rate than RMSD based methods (Wolber & Langer, 2005).

For this work all three approaches offered by Ligand Scout were used and the results were compared and combined as overlapping virtual screening results generated by different approaches have a higher chance of being a true positive.

The virtual screening results will extend the scope of the experimental data which can be considered for choosing or excluding compounds in future experiments.

Chapter 2: Methods

2.1 Two-electrode voltage-clamp electrophysiology

The two-electrode voltage-clamp electrophysiology protocol was performed similar as described in Simeone et al. (2017).

After incubation in 1 mg/ml collagenase (Sigma- Aldrich, St. Louis, MO, USA)/1ml of Oocytes (*Xenopus laevis*), the cells were defolliculated by using a glass Pasteur pipette with a fitting diameter. Subsequently the cells were injected with the mRNA (41,4 nl of either α1β3, α1β3N265S, α1β3N41R, α1β1) and incubated at 18 °C in NDE medium (96 mM NaCl, 2 mM KCl, 1 mM MgCl2, 5 mM HEPES, 1.8 mM CaCl2; pH 7.5, 100 U/ml penicillin, 100 µg/ml streptomycin, 2.5 mM pyruvate). After at least 48 hours of incubation time and with a medium change every 24 hours, electrophysiological measurements were performed.

The cells were placed in a bath with a nylon grid and impaled by 2 microelectrodes (R =~ 2 MΩ), filled with 2 M KCL. A flow of NDE constantly washed the oocytes and by a switch mechanism, various concentrations of GABA diluted in NDE could be applied. After exposure to GABA the oocytes were washed with fixed wash out times depending on the GABA or compound concentration applied.

For the measurement protocol two measurements of applying NDE with GABA only (blank) were performed at first. Then one measurement with a solution that has the same GABA concentration as the blank and diluted with a compound was applied. Lastly another blank was applied to check if the cells response is still the same as before applying the compound. The modulation induced by the compound was calculated as the fold-difference between the second blank and the compound measurement.

Following GABA concentrations were used for the blank: α1β3 (0.4 µM), α1β1 (0.4 µM), α1β3N265S (0.35 µM), α1β3N41R (0.4 µM).

For the compound 10 µM were used in addition to the GABA concentration of the blank.

The recordings were performed at room temperature and with a fixed holding potential at -60 mV. The instrument used was a Warner OC-725C two-electrode voltage clamp (TEV) (Warner Instrument, Hamden, CT, USA) and the data was digitized by a Digidata 1550 data acquisition system (Axon Instruments, Union City, CA, USA). The acquisition and data processing were performed using Clampex 10.5 (Molecular Devices, Sunnyvale, CA, USA) and Clampfit 10.5

respectively. Data analysis was performed in Graph Pad Prism 8 and statistical significance between the receptor sub types for each compound was calculated by a mixed effect model followed by a Tukey's multiple comparison test. *p < 0.05; **p < 0.01; ***p < 0.001.

2.2 Ligand Scout

For all virtual screening approaches (detailed descriptions following pages) in ligand scout following PDB structures were downloaded and used: 6X3V, 6HUP, 6HUO. The approaches were performed very similar as described in the ligand scout manual. All steps were performed with default settings and the final screening step was always kept as strict as possible. A graphical depiction of how the approaches work can be viewed in the result section in **Figure 14**.

A large database of known PQs was used for the screening. Included PQs and their substitutions can be seen in appendix **Table 5**.

2.2.1 Approach 1

For approach 1 the structure 6X3V was loaded into the structure-based view and a pharmacophore based on the native ligand etomidate (ligand name: [A] V8D_406) was generated. The pharmacophore was copied into the screening perspective and the screening was performed (**Table 1**).

2.2.2 Approach 2

For approach 2 the compounds (PZII-028, DCBS120, DCBS199, DCBSPU51, DCBSPU53, LAU176, LAU177) were loaded into the ligand-based perspective. Subsequently all compounds that show reduced efficacy in α1β3N265S mutant (DCBSPU53, LAU176, LAU177) were set to training and the other ones to ignore. The function "create pharmacophore" was used which creates a pharmacophore based on the training set. The pharmacophore was than copied to the screening perspective and the screening performed. For DCBS120 which shows decreased efficacy in the α1β3N265S mutant, the pharmacophore was generated in the structure-based perspective because in the ligand-based perspective a pharmacophore can only be generated from at least 2 molecules. The pharmacophore was again copied to the screening perspective and the screening performed.

2.2.3 Approach 3

For approach 3 the original ligand (PDB name: [A] V8D_406) was deleted from the binding site and the feature "minimize energy of side chains" was used. The compounds (PZII-028, DCBS120,

DCBS199, DCBSPU51, DCBSPU53, LAU176, LAU177) were imported in the ligand perspective and energy minimized. Then injected as library into the empty binding site. The docking was performed with AutoDock4 with default settings. After docking, binding affinity score was calculate.

Pose selection for pharmacophore-based screening

To identify good pose selection criteria and validate approach 3, a small validation protocol was performed. Known ligand-protein complexes (6HUP [D] DZP2001, (6HUO) [D] 08H501, (6X3V) [A] V8D406) were downloaded and their native ligand were re- docked. Based on the results of the redocking, which can be seen in appendix **Figure 21** and **Table 6**, two attributes were chosen which seem to reflect correctly redocked poses. In the case of the validation data set (**Table 6**) the attributes “estimated binding energy (kcal/mol)” and “binding affinity score” seem to be good indicator for correct poses.

For the PQ docking-pose-selection two poses were selected, the pose with the best scored “estimated binding energy (kcal/mol)” and the pose with the best scored “binding affinity score”. Selected poses and their pharmacophores are depicted in the result section **Figure 16** (detailed docking data appendix **Table 7**).

The pharmacophores were then used from compounds that show reduced efficacy in the α1β3N265S mutant (DCBSPU53, LAU176, LAU177) to perform the screening process (detailed data appendix **Table 8)**.

Chapter 3: Results

3.1 Data Overview

Experiments were performed at 10 µM compound concentration and ~ GABA EC5. Fold modulation was calculated as fold difference from compound + GABA in comparison to a control blank (only GABA). See **Figure 5** for a summary of the results.

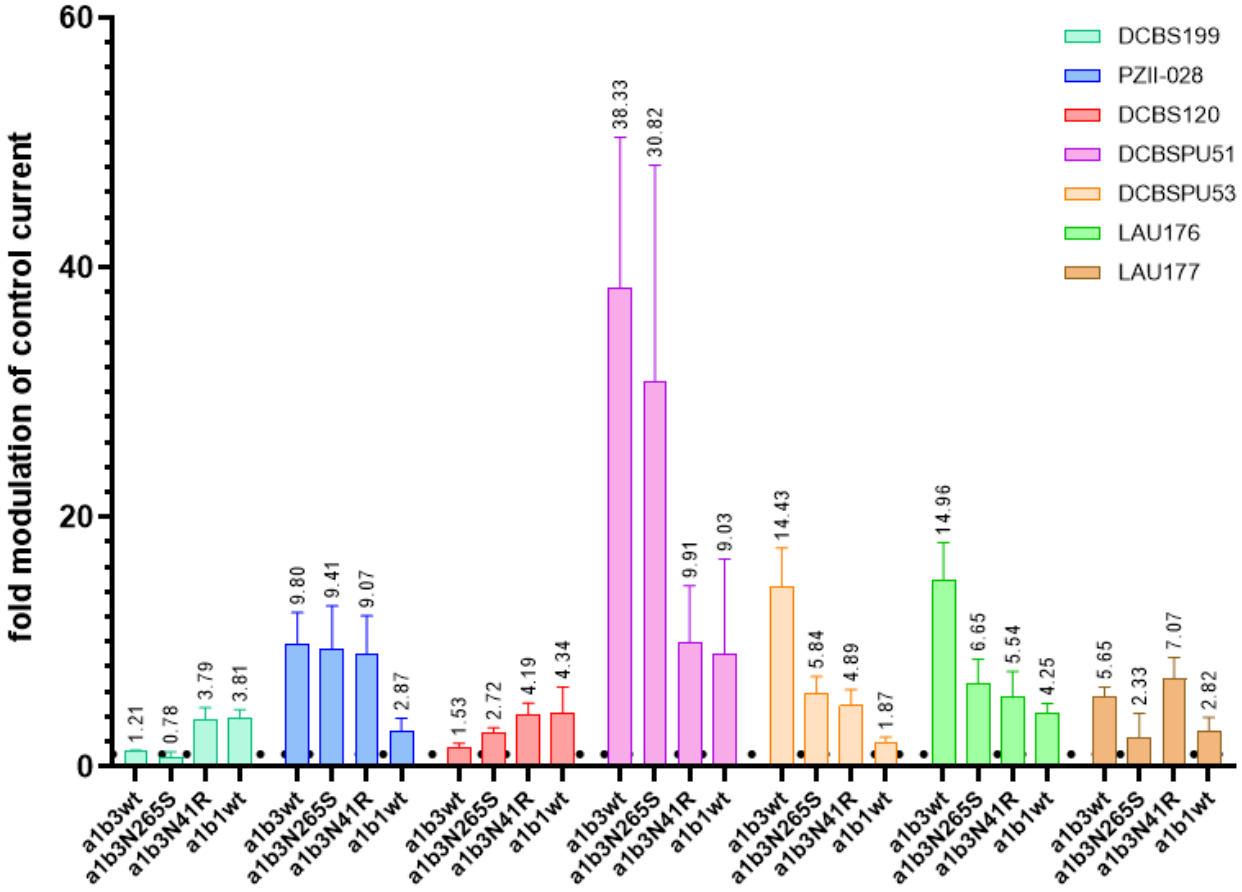

Figure 5 | Overview of Experimental Data and individual PQs effect (fold modulation of control current - mean with sd, n=4-6/compound/receptor subtype) measured by voltage clamp

DCBS199 (R8 = Cl, R'4 = NHAc)

DCBS199 is substituted with a chlor atom on position R8 and an acetylated amino group on position R'4. It is not or weakly modulating α1β3 wildtype receptors with an efficacy of 1.2-fold (1.21 ± 0.08) increase in currents and also not modulating α1β3 N265S receptors with an efficacy of 0.78-fold (0.78 ± 0.42) decrease in currents. The modulation in α1β1 wildtype is much higher with a 3.8-fold (3.81 ± 0.76) increase in currents. The difference between α1β1 wildtype and α1β3 wildtype is significant (p = 0.068) and the difference between α1β1 wildtype and α1β3

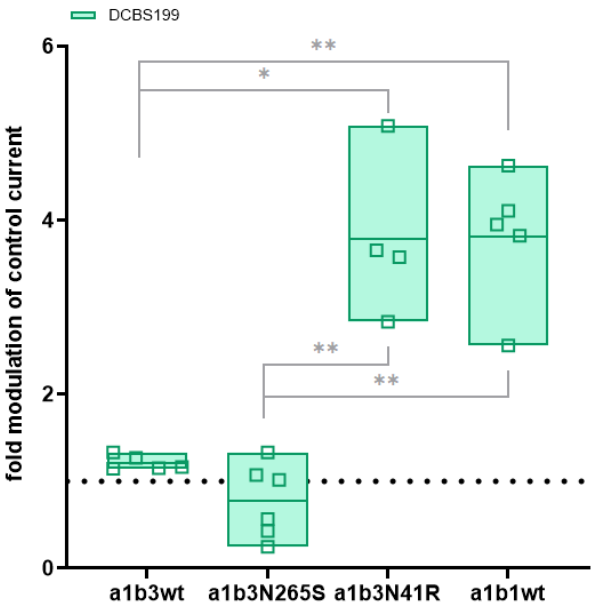

Figure 6 – Boxplot for DCBS199

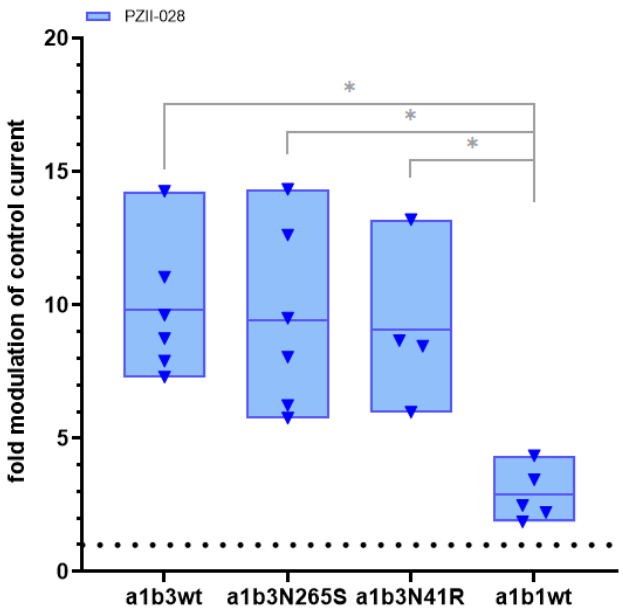

Figure 7 – Boxplot for PZII-028

N265S is significant (0.0021). α1β3 N41R receptor variant also shows a similar positive allosteric modulation as α1β1 wildtype with a 3.8-fold (3.81 ± 0.76) increase in currents. Again, the difference between α1β3 N41R and α1β3 wildtype is significant (p = 0.0324) and the difference between α1β3 N41R and α1β3 N265S is also significant (p = 0.0097).

PZII-028 (R8 = Cl, R'4=OMe)

PZII-028 substituents are chloro at position R8 and a methoxy group at position R'4. The efficacy in α1β3 wildtype (9.80 ± 2.55), α1β3 N265S (9.40 ± 3.46) and α1β3N41R (9.07 ± 3.01) is very similar and around 9-fold increase in currents. The efficacy in α1β1 wildtype is lower with around 2.9-fold increase (2.87 ± 1.01). The difference between α1β3 wildtype (p = 0.0330), α1β3 N265S (p = 0.0341) and α1β3N41R (p=0.0462) compared to the α1β1 wildtype is significant.

DCBS120 (R8=Cl, R'3=NH4)

DCBS120 is substituted with a R8 chlor and a R'3 ammonium group. It is very weak positive allosteric modulator in α1β3 wildtype receptors with an efficacy of 1.5-fold (1.53 ± 0.33) increase in currents. The α1β3 N265S shows a similar efficacy of about 2.7-fold (2.72 ± 0.42) increase in currents. There is a significant difference (p = 0.0331) in the α1β3 N41R with a modulation of 4.2-fold (4.188 ± 0.91) compared to the α1β3 wildtype. The difference induced

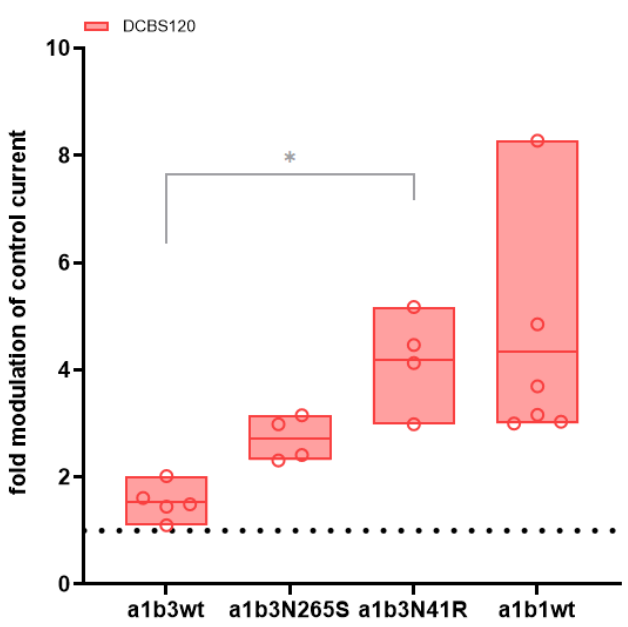

Figure 8 – Boxplot for DCBS120

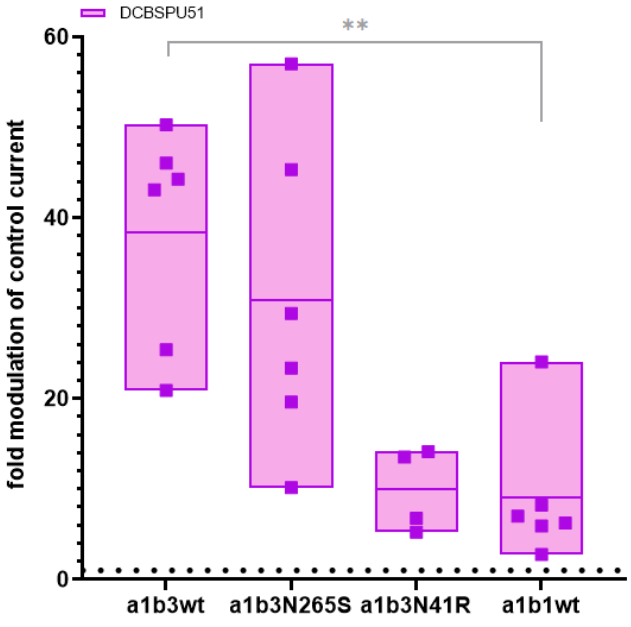

Figure 9 – Boxplot for DCBSPU51

by the N265S mutation is nearly significant (p = 0.0572). The α1β1 wildtype also shows a higher modulation compared to the a1b3 wildtype with 4.3-fold (4.34 ± 2.05) increase in currents although not significant (p = 0.0917) due to a higher variation induced by a value that deviates from the other other values but not far enough to be a statistical outlier (**Figure 5**).

DCBSPU51 (R8 = Cl, R6 = tBu, R'4 = OMe)

DCBSPU51 is structurally very similar to DCBSPU53 with chlor on position R8 and methoxy on position R'4 but instead of ethyl it is substituted with isopropyl on position R6. Its efficacy in α1β3 is the highest from all observed PQs with an increase in currents about 40-fold (38.34 ± 12.09) but it also shows the highest variation. The efficacy in α1β1 wildtype is much lower with 9-fold increase of currents (9.03 ± 7.59) and the difference compared to α1β3 is significant (p = 0.099). The α1β3N265S mutation shows a similar high positive allosteric modulation by the compound as the α1β3 wildtype with a 30-fold increase in currents (30.82 ± 17.35) and shows a lot of variability. The α1β3N41R induces much lower positive modulation of 9-fold (9.91 ± 4.58) but the difference is not significant, yet very close (p = 0.0594).

DCBSPU53 (R8 = Cl, R6 = Et, R'4 = OMe)

DCBSPU53 is substituted with a chloro on position R8 but comes with an additional ethyl substituent at position R6 on ring A. It is a very strong positive allosteric modulator in α1β3 wild

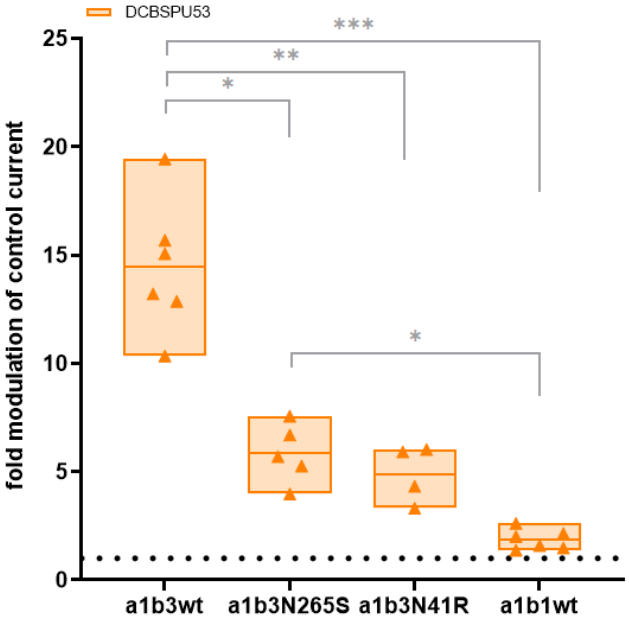

Figure 10 – Boxplot for DCBSPU53

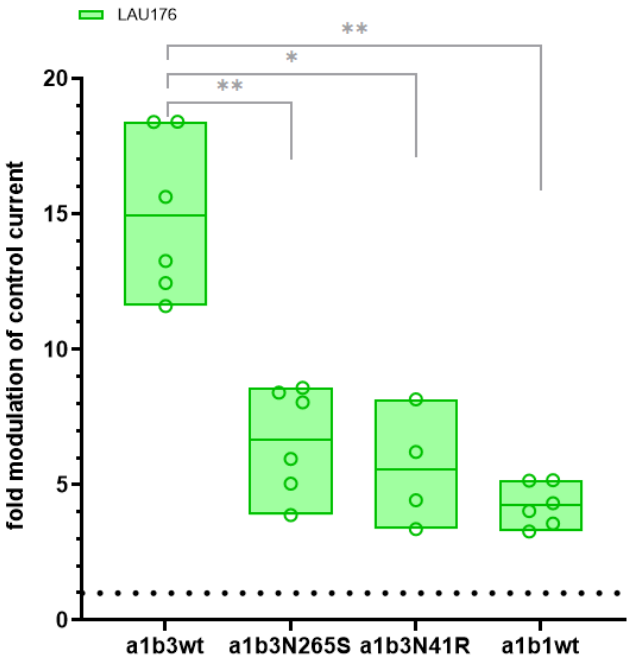

Figure 11 – Boxplot for LAU176

type receptors (**Figure 5**) and enhances GABA mediated currents about 15-fold (14.43 ± 3.09). In α1β1 it enhances currents about 1.87-fold (1.87 ± 0.48). The difference between α1β3 and α1β1 is significant (p = 0.0008). The α1β3 N265S mutation in the TMD significantly (p = 0.0057) reduces the efficacy from about 15-fold to 6-fold (5.84 ± 1.38). Lastly the α1β3N41R mutation in the ECD also reduces the efficacy to 5-fold (4.89 ± 1.31) and the reduction is significant (p = 0.0468).

LAU176 (R8 = OMe, R'4 = OMe)

LAU176 comes with two methoxy substituents, one on position R8 and one on position R'4. It is a strong positive allosteric modulator in α1β3 wildtype receptors (**Figure 5**) and enhances currents 15-fold (14.96 ± 2.99) and a much weaker one in α1β1 wildtype (4.25 ± 0.79). The difference is significant (p = 0.0029). Efficacy is significantly reduced in the α1β3N265S receptors (6.65 ± 1.97, p = 0.0071) and α1β3N41R receptors (5.54 ± 2.10, p = 0.0319).

LAU177 (R8 = OMe, R'4=CN)

LAU177 has a chlor substituent at position R8 and a nitrile group at position R'4. The efficacy in α1β3 wildtype is 5.7-fold (5.65 ± 0.73) increase in currents. A significant drop (p = 0.0398) in efficacy can be observed in the α1β3 N265S receptors to 2.3-fold (2.33 ± 1.95) and a not significant (p = 0.0552), but very close to significant, difference in the α1β1 receptors with a

2.8fold (2.82 ± 1.14) increase in currents. The α1β3 N41R variant shows a 7-fold (7.08 ± 1.65) increase in currents compared to GABA alone.

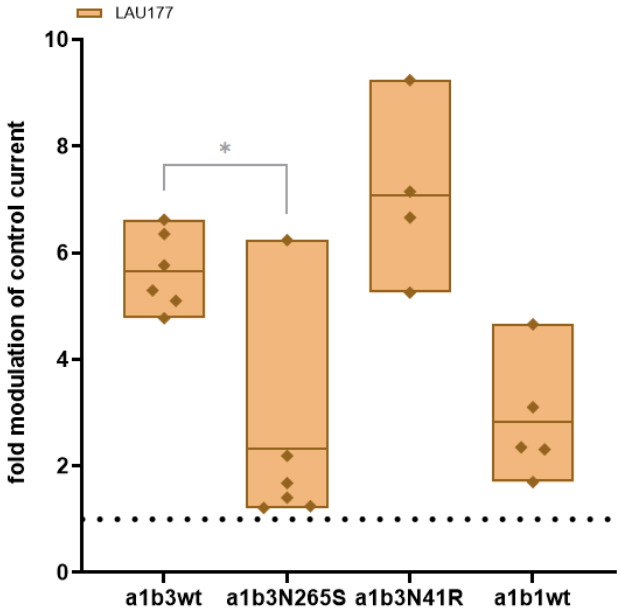

Figure 12 - Boxplot for LAU177

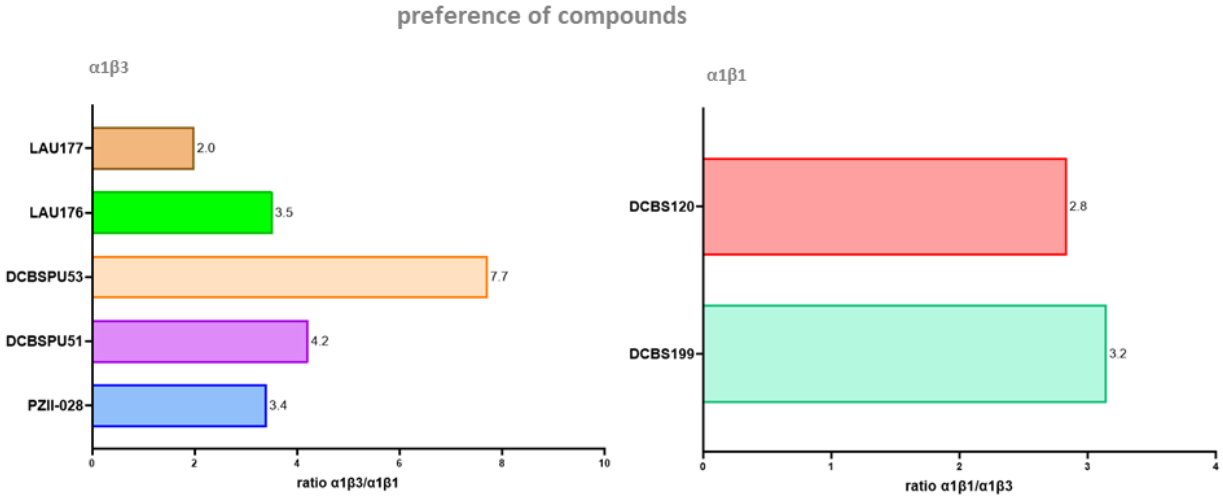

Figure 13 – preference of compounds for α1β3 and α1β1 depicted as fold difference in efficacy for the dominant receptor type

3.2 α1β3 preferring compounds – ECD + TMD influenced

3.2.1 DCBSPU53

The most α1β3 preferring compound is DCBSPU53. The efficacy is 7.7 times higher in α1β3 than it is in α1β1. It is affected by the N265S as well as the N41R point mutation hence it is probably using both binding sites to generate the efficacy in α1β3. The efficacy in α1β1 is the lowest when compared to the other measured compounds.

3.2.2 LAU176

The compound LAU176 seems to behave very similar to DCBSPU53 regarding binding site usage and α1β3 selectivity although its α1β3 selectivity is much lower with a 3.5 times higher modulation in α1β3.

The results are in line with Maldifassi et al. (2017) where he showed a strong reduction of efficacy in α1Y209Qβ2γ2 receptors. In these receptors binding to the ECD α+/β- Interface as well as to the α+/γ- Interface seem to be inhibited and this might cause the reduction of efficacy when compared to α1β2γ2 wildtype. The compound might use both ECD Interfaces since the reduction he measured is greater than the reduction measured in α1β3N41R receptors which are missing the α+/γ- Interface.

Also, Simeone et al. (2017) showed similar efficacy data for this compound in α1β3 wildtype, α1β3N41R and α1β1 wildtype receptors.

3.3 α1β3 preferring compounds – ECD dominant

3.3.1 DCBSPU51

The compound DCBSPU51 shows a preference for α1β3 wildtype receptors with a 4.2 times higher modulation however the efficacy in α1β1 wildtype is with about 10-fold modulation way too high to be useful as a α1β3 preferring compound. The α1β3N41R reduces the efficacy to a similar value as in the α1β1 wildtype receptors so this compound might generate a large part of its efficacy via the ECD α+/β- Interface. Still due to high variation in the data the influence of the α1β3N265S mutation cannot be evaluated.

3.4 α1β3 preferring compounds – TMD dominant

3.4.1 LAU177

LAU177 seem to show preference for α1β3 with a 2 times higher modulation compared to α1β1. Since the N265S mutation reverts the α1β3 efficacy to a similar amount as in α1β1 and the N41R mutation generates no change at all, the TMD β+/α -Interface seem to be the main binding site for this compound.

Previous data by Maldifassi et al. (2016) shows similar trends for LAU177. When mutating the β2N265 amino acid to I in α1β2γ2 receptors a nearly complete reduction of efficacy was observed. He also found a small but significant reduction in efficacy in α1Y209Qβ2γ2 receptors. The α1Y209Q might affect binding to the ECD α+/β- Interface as well as binding to the ECD α+/γ- Interface. In conclusion two possible explanations might be possible when summing up the available data: Since the data for LAU177 gathered for this work (**Figure 12**) shows quite some variation in the α1β3N41R receptors, it might be possible that the compound binds the ECD α+/β- Interface and generates a minor part of its efficacy via this site as observed in Maldifassi's work. The other explanation might be that the reduction in efficacy Maldifassi observed, is induced by the mutated α+/γ- Interface since the α1Y209Q mutation might also affect binding to this site.

3.5 α1β3 preferring compounds – not influenced by mutations

3.5.1 PZII-028

The compound PZII-028 also shows α1β3 preference with a 3.4-fold higher modulation. Neither the N265S nor the N41R mutation is affecting the efficacy in α1β3 in a significant way.

However, Simeone et al. (2017) found a significant reduction in efficacy of PZII-028 when comparing the efficacy in α1β3 wildtype with the efficacy in the α1β3N41R mutant and when considering the high variation of this compound in this works experimental data, this compound is very likely using the ECD α+/β- Interface as indicated in Simeone et al. (2017).

Additionally other TMD sites like the α+/β- might also play a role (Maldifassi et al., 2016)

3.6 α1β1 preferring compounds – ECD dominant

3.6.1 DCBS120

DCBS120 shows a tendency towards α1β1 preference but due to a measurement that highly deviates from the mean the difference between α1β1 and α1β3 is not significant. Nevertheless, the difference between α1β3 and the N41R ECD conversion mutation to α1β1 is significant. Modulation in α1β1 is 2.8-fold higher and this compound seems to use dominantly the ECD Interface.

3.6.2 DCBS199

The compound DCBS199 not only shows α1β1 preference but selectivity with a 3.2-fold difference and no modulation at all in α1β3. While the N265S mutation shows no difference in efficacy the N41R mutations completely restores α1β1 efficacy.

Both compounds are substituted with a chloro atom on position R8 and have a amino substituent on ring D in common, although on different positions.

3.7 Computational Work

To expand the scope and the interpretation of the experimental data, Ligand Scout was chosen as a computational toolbox. The experimental data was used to find patterns and similarities in pharmacophores and a library of known PQs was screened (appendix **Table 5**). For that purpose, three different approaches were chosen (**Figure 14**).

Approach 1 – using the etomidate pharmacophore

The results of the pharmacophore screen based on etomidate pharmacophore (for details go to methods) are depicted in **Table 1**. The screen was performed with completely strict settings and required matching all etomidate pharmacophore features.

With a pharmacophore-fit-score of 36.91 the compound DCBSPU53 was matched which is in line with the experimental data. Additionally CGS9895 was also matched with the etomidate pharmacophore and is known to be influenced by mutations in the α1β3 TMD interface

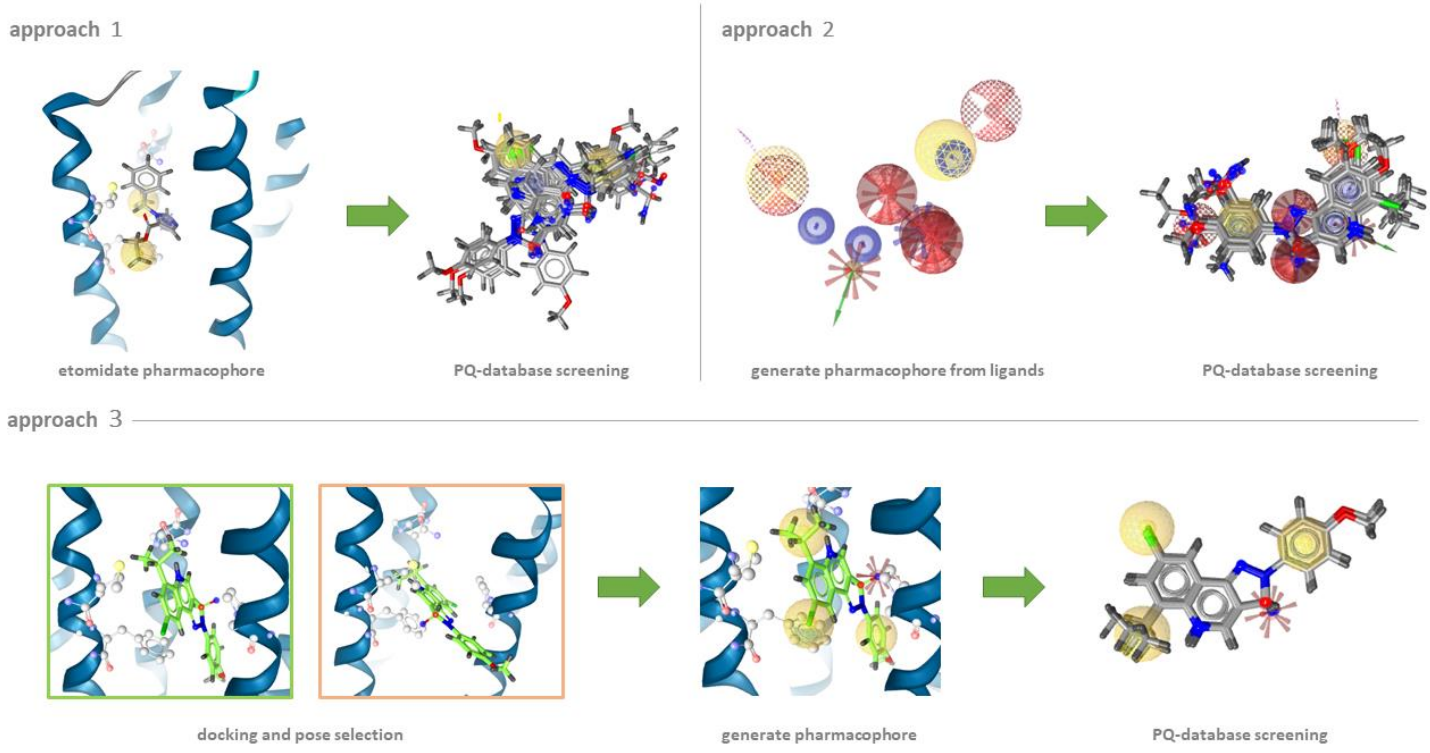

Figure 14 – depicted are the three approaches that were used for the virtual screenings. Approach 1 – structure-based pharmacophore from etomidate (PDB structure: 6X3V). Approach 2 – ligand-based pharmacophore from DCBSPU53, LAU176 and LAU177. Approach 3 – structure-based pharmacophore generated by docking DCBSPU53, LAU176 and LAU177 into etomidate pocket (PDB structure: 6X3V)

(Maldifassi et al., 2016).

Also, preliminary data from DCBSPU21 (appendix **Figure 22**) is indicating that it might bind to the α1β3 TMD Interface and is recognized.

In contrast to some true positive matches, also DCBS152A (appendix **Figure 22**) and DCBS120 (**Figure 5**, **Figure 8**) are matched with the etomidate pharmacophore but for them existing experimental data is not confirming that these compounds show decreased efficacy in α1β3N265S receptors.

For the other matches there is no data available but considering the confirmed true positive matches and their better scored pharmacophore fit scores (**Table 1**) some of the top scored matches (XHEIII006C, PZII029, XHEIII063, PWZ009A1, CGS9896, LAU165, CGS8216) might have a high chance of being α1β3 TMD β+/ α- interface binders.

PQ	PH4-Fit Score
XHEIII006C	38.12
PZII029	38.12
XHEIII063	37.88
PWZ009A1	37.76
CGS9896	37.65
CGS9895	37.65
LAU165	37.58
CGS8216	37.51
DCBSPU53	36.91
DCBS152B	36.81
DCBS119	36.57
LAU462	36.43
DCBS152A	36.31
DCBSPU51	36.29
DCBSPU21	36.18
LAU159	36.11
DCBS146	36.07
XHEII17	36.05
DCBS142	36.02
DCBS32	35.96
DCBS120	35.89

Table 1 – Screening results - etomidate pharmacophore, green – true positive, blue – might be true positive, yellow – might be false positive, red – false positive

Approach 2 – ligand-based pharmacophore

For the second approach PQs that show a significant decrease in modulation induced by the N265S TMD mutation were used to generate a ligand-based pharmacophore model.

The PQs used for this model (model 1) where DCBSPU53, LAU176 and LAU177. Additionally, the compound DCBS120 was also used to generate a separate pharmacophore model (model 2) since it is showing a nearly significant ($p = 0.0572$) increase in modulation in the N265S converted receptors.

To sum it up, it was differentiated between compounds that show reduced efficacy in the N265S mutated receptors and compounds that show increased efficacy in these receptors when compared with α1β3 wildtype. The compounds superimposed with their pharmacophore can be seen in **Figure 15**. The library of PQs (appendix **Table 5**) was then screened for a pharmacophore fit to pinpoint PQs with a potential similar TMD binding behaviour.

The pharmacophore features of model 1 are composed of either a hydrogen bond acceptor or negative ionizable area on position R'4 on ring D and either a lipophilic feature or a hydrogen bond acceptor on position R8 on ring A. The hydrogen bond acceptor feature is in most cases a

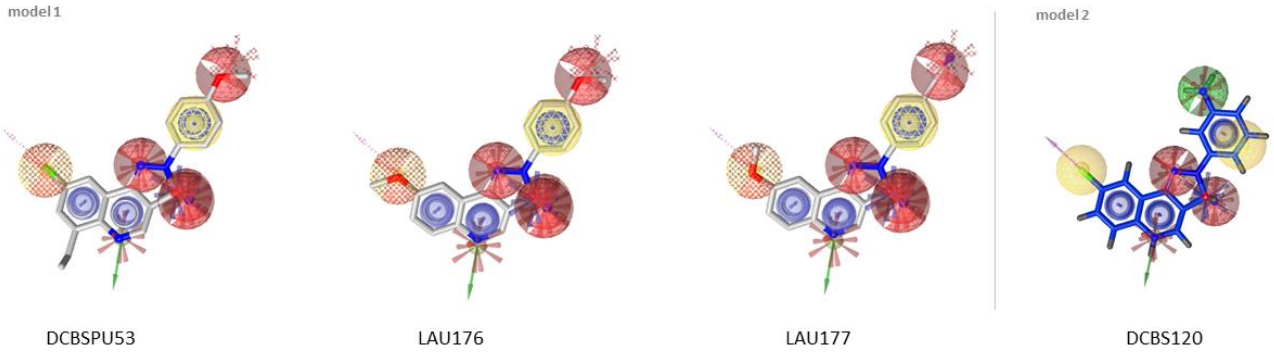

Figure 15 –PQs influenced by TMD mutations and superimposed with the generated pharmacophore models

methoxy substituent (DCBSPU53, LAU176) and in one exception, the nitrogen from a nitrile substituent (LAU177). Additionally, the nitrile substituent from LAU177 holds a negative ionizable area. The common denominator seems to be the R'4 hydrogen bond acceptor feature on ring D.

To reduce the false positive rate, the results were manually filtered to have at least one of the possible features on Ring A (lipophilic or hydrogen bond acceptor) and at least one of the two possible features on Ring D (hydrogen bond acceptor or negative ionizable

area).

The results are depicted in **Table 2**. Again, DCBSPU21 was matched and in addition also DCBS128. Both have preliminary data showing that they might have reduced efficacy in the N265S mutant receptors (appendix **Figure 22**).

Additionally, two molecules for which preliminary data show that they are not influenced by the mutation are matched. DCBSPU27 is a compound like DCBSPU21 with only one difference, a chloride substituent on position R6 instead of a fluoride substituent (for substituents see appendix **Table 5**) so one might hypothesize that the chloride groups bigger size induces the difference in binding behaviour. DCBS93 has a NO2-substituent at position R'4 where the two oxygens function as hydrogen bond acceptor but since they are slightly dislocated when compared to the original pharmacophore this might explain the difference in binding behaviour. Both potential false positives appear towards the bottom of the list sorted by pharmacophore fit score.

Model 2 consists of either a hydrogen bond donor feature or a negative ionizable area feature on position R'3 and a lipophilic feature on position R8.

The subsequent screening was again filtered to match the R8 feature (lipophilic feature) and one of the R'4 features (hydrogen bond donor or negative ionizable area). The results can be seen in **Table 3**.

The best match DCBS152B, matches both features on Position R'3 and chances are high that it shows a similar behaviour as DCBS120.

For the second-best results, DCBS152A there is preliminary data (appendix **Figure 22**) available which shows a slightly increased efficacy in the α1β3 N265S receptors compared to α1β3 wildtype but the difference in efficacy and the n number is too small to draw a meaningful conclusion.

Approach 3 – docking PQs into the TMD Interface

Lastly a docking-based approach was used. TMD binding PQs that show reduced efficacy in the α1β3N265S (DCBSPU53, LAU176, LAU177) were docked into the structure 6X3V (for details go to methods) by AutoDock4 using Ligand Scout.

Prior to docking the PQs, a small validation protocol was performed to see how well the docking via AutoDock4 in Ligand Scouts can restore correct docking poses in known ligand-protein complexes from the PDB (appendix **Table 6**, **Figure 21**). AutoDock4 performed very well in restoring correct docking poses and the attributes "estimated binding energy (kcal/mol)" and "binding affinity score" seem to be good indicators for corrects poses. In every restored docking pose at least one of both values was ranked as the highest in a relative perspective over all generated poses for the respective ligand.

Name	PH4-Fit Score
LAU161	152.43
DCBSPU53	149.23
LAU462	149.19
DCBSPU51	149.19
PZII028	149.18
DCBSPU26	149.18
LAU177	146.02
XHEIII24	145.99
LAU176	142.79
DCBS128	142.16
LAU162	141.79
DCBSLK36	141.79
DCBSPU21	141.78
DCBSPU27	141.77
DCBSPU19	141.76
LAU157	139.04
DCBS119	138.69
DCBSLK60	136.15
PZII029	136.07
DCBS88	135.8
DCBS93	132.64
DCBS52	131.93

Table 2 – Screening results – Model 2, blue – might be true positive, yellow – might be false positive, grey – source of ph4

Name	PH4-Fit Score
DCBS120	159
DCBS152B	157.54
DCBS152A	148.57
DCBS146	147.97

Table 3 – Screening results – Model 1, grey – source of ph4

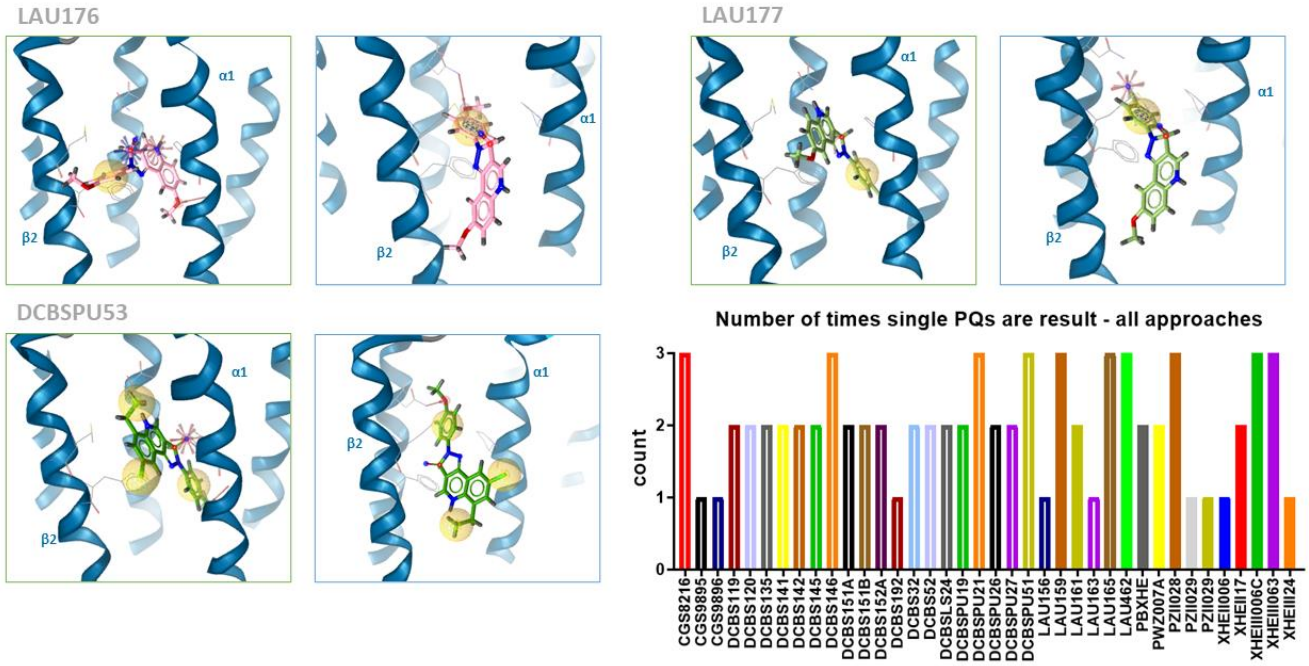

Figure 16 – TMD binding PQs and their two best scored docking poses as ranked by either Binding Energy (kcal/mol)(green border), or by Binding Affinity Score (blue border). Right/bottom: number of times PQs are appearing summed up over all 3 approaches

After docking of the PQs, the generated docking poses were then filtered by following criteria: The first criterium was that the ligand had to be in proximity of the N265 amino acid inside the pocket. Then the pose with the best "estimated binding energy (kcal/mol)" and the pose with the best "binding affinity score" per PQ was used as a template for generating two pharmacophores for the subsequent screening steps. The selected poses and their generated pharmacophores for the screening steps are depicted in **Figure 16.** The results of the screening steps can be viewed in the appendix **Table 8**.

The weakness of approach 3 is that it is based on structure-based-pharmacophores generated by theoretical docking poses. Nevertheless, and shown in the small validation protocol (appendix **Table 6**, **Figure 21**) some of these poses might reflect actual poses.

The screening results were also summed up with the previous approaches. PQs appearing in more than one approach might have a higher chance of being a true positive match. The results of this calculation can be seen in the graph depicted in **Figure 16** (right/bottom).

10 compounds are appearing in all three approaches. 8 of them have a hydrogen bond acceptor feature on ring D either in the R'3 (DCBS146, LAU159, LAU165) or R'4 (DCBSPU19, DCBSPU21, DCBSPU51, LAU462, PZII-028) position (details for substituents appendix **Table 5**).

Taking experimental data into account, chances are high that matched compounds with hydrogen bond acceptor feature in position R'4 are also binding the TMD β+/ α- interface.

For compounds with hydrogen bond acceptor feature on position R'3 no data exists about TMD β+/ α- interface usage.

Two compounds (XHEIII006C, XHEIII063) are not containing hydrogen bond acceptor features on Ring D. XHEIII006C has a lipophilic feature at position R'4 and XHEIII063C a lipophilic feature plus a hydrogen bond donor feature on position R'4. No data about TMD β+/ α- interface site usage of such compounds is available.

Best scored docking poses from all poses

Since approach 3 generated data about docking poses for all the PQs (PZII-028, DCBS120, DCBS199, DCBSPU51, DCBSPU53, LAU176, LAU177) analysed in this work, an additional population wide analysis of the docking poses was performed. Therefore, all docking poses were categorized and assigned to binding modes and the mean "estimated binding energy (kcal/mol)" as well as the mean "Binding Affinity" was calculated for each binding mode (**Figure 17,** appendix **Table 7**).

The two best scored binding modes ranked by mean "estimated binding energy (kcal/mol)" and mean "Binding Affinity" were chosen and are depicted in **Figure 17**.

binding PQs, namely DCBSPU53 and LAU177. For all the compounds populating binding mode 1, it is the best scored pose ranked by Binding Energy Score (**Figure 16**, appendix **Table 7**).

Pose 8 includes DCBS120 and DCBS199. Both seem not to be influenced by the α1β3 TMD interface according to experimental data which makes pose 8 less probable.

The best scored binding mode by mean "estimated binding energy (kcal/mol)" is binding mode 1 and includes DCBSPU53, DCBSPU51, DCBS120 and LAU177. It is shared by 2 of 4 confirmed TMD

The best ranked binding mode by factor "binding affinity score" is binding mode 5 which includes DCBSPU53 and DCBSPU51.

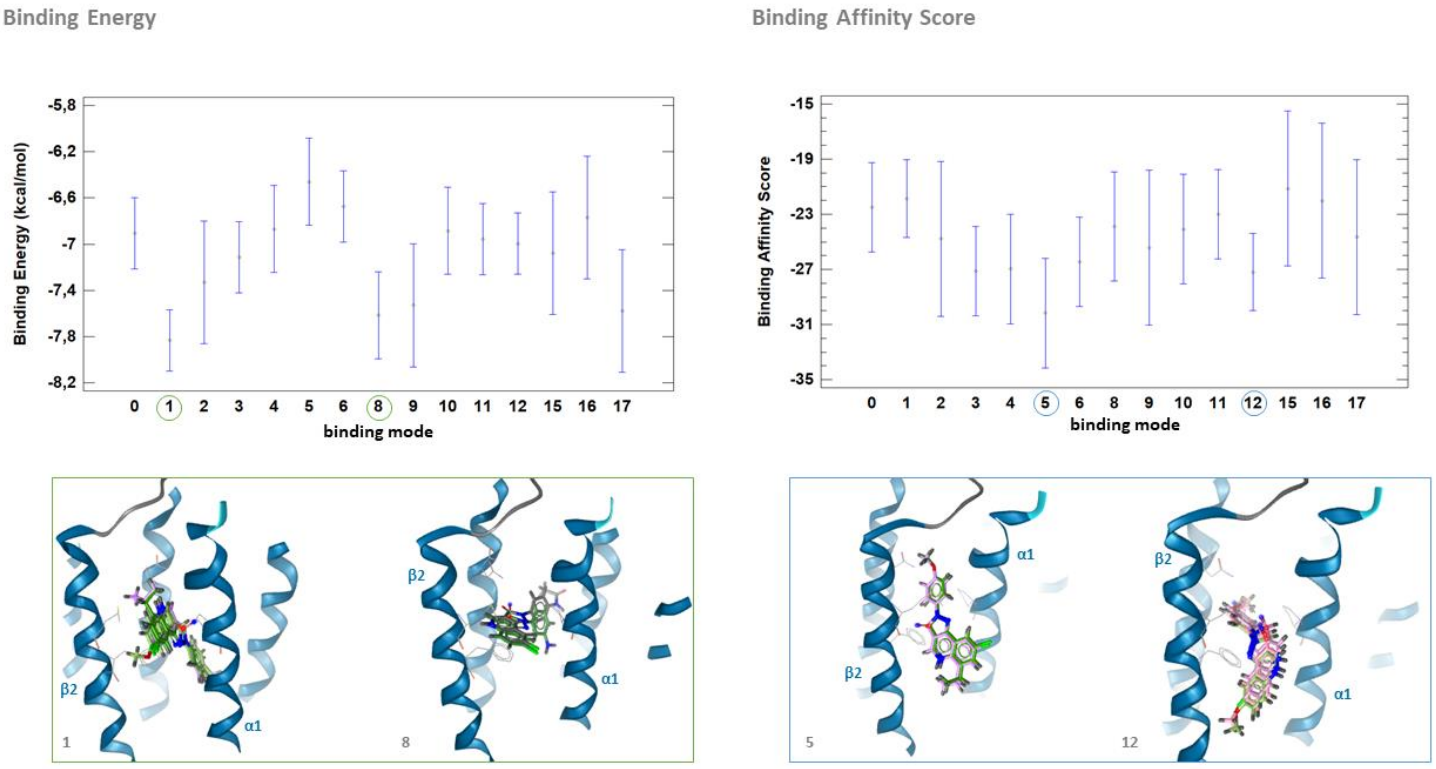

Figure 17 – Best 3 scored docking poses from all calculated poses generated by Auto Dock 4 ranked by Binding Energy and Binding Affinity Score

The second-best binding mode by factor "binding affinity score" is pose 12 which includes LAU177, LAU176, PZII-028, DCBS199. For both LAU176 and LAU177 this is the best pose by factor binding affinity score (**Figure 16**, appendix **Table 7**).

All the poses are close enough to the amino acid N265 inside the TMD binding pocket to be able to interact with it.

Since there are no available ligand-protein complexes with PQs available in the PDB this step was done to select best possible binding poses generated via Auto Dock 4 so they can be compared with docking poses generated by other docking algorithms.

Virtual screening based on Pharmacophore features of α1β1 preferring compounds

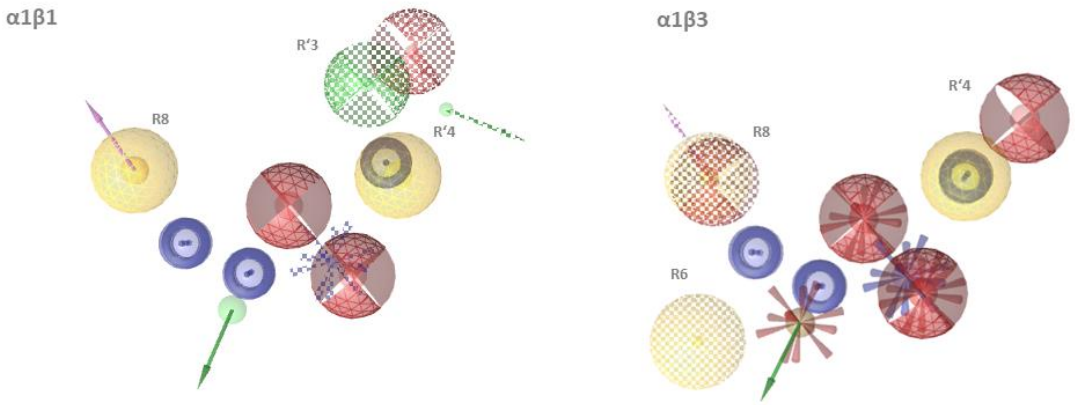

Figure 18 – pharmacophore features of α1β1 (DCBS120, DCBS199) and α1β3 (DCBSPU53, LAU176, LAU177) preffering compounds.

According to the results of the experimental data the pharmacophore features that make a PQ α1β1 preferring is a hydrogen bond donor on ring D (green pharmacophore feature, R'3, **Figure 18**) in either the R'3 or R'4 position. In the case of DCBS120 and DCBS199 the hydrogen bond donor is a nitrogen atom from an amine substituent. Based on the merged feature pharmacophore generated by both compounds and a subsequent screening, only DCBS152B matches the hydrogen bond donor feature on position R'3 and could behave in a similar way. The hydrogen bond donor feature on position R'4 oddly is not matched from any other PQ in the database via Ligand Scout screening even though there should be other PQ's like LAU206 or DCBS96 that have an amino substituent at this position. Another possible feature that drives α1β1 preference might be the hydrogen bond acceptor feature on position R'4 but further away from ring D (red pharmacophore feature, R'3, **Figure 18**) which corresponds to the oxygen of the acyl group attached to the amine substituent from DCBS199. Best scored PQs ranked by pharmacophore-fit score that are matching that feature are DCBS119, DCBS146 and DCBS152A (**Table 5**).

Virtual screening based on Pharmacophore features of α1β3 preferring compounds

The pharmacophore features generated by three of the most α1β3 preferring compounds DCBSPU53, PZII-028 and LAU176 can be seen in **Figure 18**. DCBSPU51 was not used for the pharmacophore since its efficacy is too high in α1β1 to be useful as α1β3 preferring compound.

Ring A features on position R8 can be either a hydrophobic feature like a chloro substituent or a hydrogen bond acceptor like a methoxy group. A bulky hydrocarbon on position R6 reflecting

another hydrophobic feature can also additionally be located on ring A.

Ring D seem to be more specific and on position R'4 all three are possessing an electron bond acceptor. The results of the screen are depicted in **Table 4** and sorted by pharmacophore-fit-score.

All of them match the hydrogen-bond acceptor feature on position R'4 and for LAU462, XHEIII24 and PZII-029 efficacy data for α1β3 exists and are showing decent modulation in these receptors (2-fold-4-fold) (Fabjan et al., 2021).

Table 4 – Screening result for α1β1 and α1β3 preffering compounds

Ligand	PH4-Fit-Score	PH4
DCBS152B	111.92	a1b1-pref.
DCBS119	107.92	a1b1-pref.
DCBS146	107.34	a1b1-pref.
DCBS152A	107.31	a1b1-pref.
DCBSPU21	137.56	a1b3-pref.
DCBSPU27	137.54	a1b3-pref.
DCBSPU53	137.53	a1b3-pref.
DCBSPU19	137.51	a1b3-pref.
LAU462	137.5	a1b3-pref.
DCBSPU51	137.5	a1b3-pref.
DCBSPU26	137.49	a1b3-pref.
LAU161	137.28	a1b3-pref.
XHEIII24	132.5	a1b3-pref.
LAU177	132.2	a1b3-pref.
PZII029	127.59	a1b3-pref.

Chapter 4: Discussion and Conclusion

4.1 Many PQs seem to use the TMD interface

Compounds that show significant influence ($p < 0.05$) induced by the TMD α1β3 N265S mutation are DCBSPU53, LAU176, LAU177. DCBS120 shows nearly significant ($p = 0.0572$) influence.

DCBSPU53, LAU176 and LAU177 have significantly reduced efficacy in α1β3 N265S compared to α1β3 wildtype which means that they probably use the α1β3 TMD interface. For DCBS120 the conversion mutation of the TMD interface to α1β1 increases the efficacy meaning that it might bind the α1β1 homologue of this interface.

DCBSPU51 shows high variation in the experimental data and no significant influence by the TMD α1β3 N265S mutation yet a trend towards being influenced by it. Considering that the pharmacophore overlaps completely with DCBSPU53 and it is appearing in all three virtual screening approaches it could be able to interact with that binding site and further data might be needed to confirm it.

It seems that there is a tendency for compounds that show a high efficacy and preference for α1β3 to be strongly influenced by the α1β3N265S conversion mutation. The overlapping features of molecules behaving that way seem to be a substituent at position R'4 acting as a hydrogen bond acceptor. In the case of DCBSPU53, LAU176 it is the methoxy substituent and in the case of LAU177 the nitrile substituent. Another differentiation by effects can be made between R'4 methoxy and nitrile substituted compounds. While the methoxy substituted compounds are also influenced by the ECD α1β3N41R mutation, the nitrile substituted compound LAU177 is not, still previous data by Maldifassi et al. (2016) showed minor influence of a mutation involving the ECD α+/β- and ECD α+/γ- interface. The data in this works is too variable to show the involvement of the ECD α+/β- interface. Despite this it is also possible that the compound LAU177 also uses the ECD α+/γ- interface for a minor part of its PAM effects, which would be in line with affinity data showing affinity for the ECD α+/γ- interface in α1β3γ2 receptors (Varagic et al., 2013).

Ring A substitutions on position R8 seem to be more heterogenous in terms of TMD binding capability of compounds. R8 can be a hydrogen bond acceptor like a methoxy or a lipophilic feature like the chloride substituent. Compounds with lipophilic hydrocarbons located at position

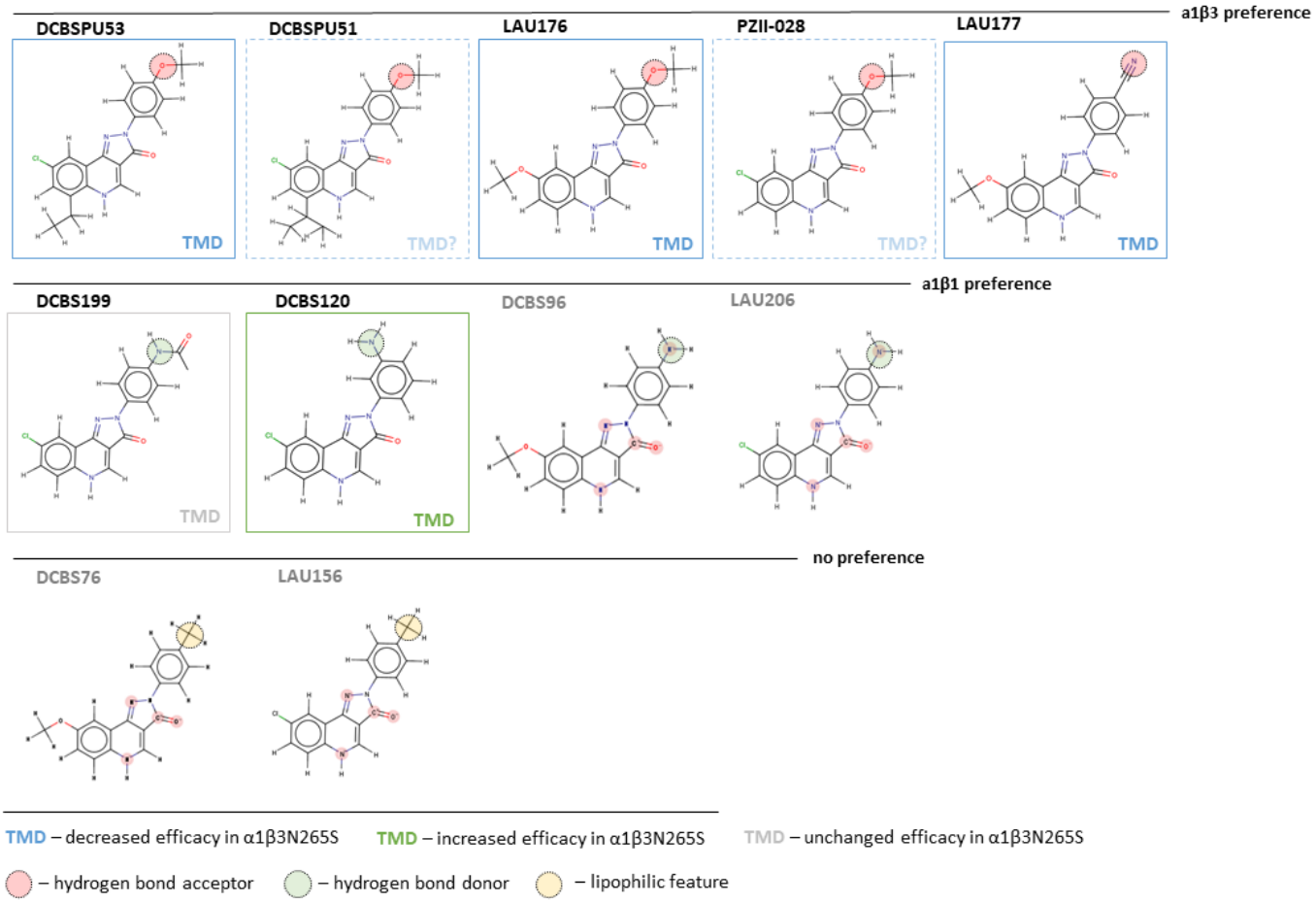

Figure 19 – PQs sorted by receptor subtype preference (left to right ordered by highest fold ratio of preference). black names: data from this work, gray names: data from Simeone et al. (2017). No borders – no data for TMD binding, dashed border – preliminary data exists but more data needed

R6 can also interact with the TMD Interface and in the case of DCBSPU51, the larger hydrocarbon substituent (isopropyl) seem to boost the efficacy of the otherwise very similar molecule.

For DCBS120 which seems to bind the α1β1 converted TMD interface the pharmacophore features are a hydrogen bond acceptor and a negative ionizable area on position R'3 and a lipophilic feature on position R8.

It seems that ring D plays a more important role influencing the TMD binding behaviour.

4.2 Five compounds show α1β3 preference

The five a1b3 preferring compounds, meaning that they show higher efficacy in α1β3 wildtype receptors in contrast to α1β1 are DCBSPU53, DCBSPU51, LAU176, PZII-028 and LAU177 (**Figure 19**). The most prominent pharmacophore features of this group of compounds are the R'4 methoxy substituent on Ring D which four of them have. LAU177 is the only exception having a

nitrile substituent on position R'4. Both type of substituents are capable of functioning as a hydrogen bond acceptor pharmacophore feature which taken together makes the hydrogen bond acceptor feature on position R'4 the common denominator of compounds behaving α1β3 preferring.

Position R8 on Ring A seem to play less of a specific role since two types of pharmacophore features can be observed, either a lipophilic feature or a hydrogen bond acceptor feature.

Three of the α1β3 preferring compounds also show reduced efficacy in α1β3N265S converted receptors so partly the higher efficacy in α1β3 wildtype receptors might come from these group of compounds being able to bind to both interfaces, the ECD and the TMD interface and thereby generating the increased efficacy, maybe even trough allosteric effects of both binding sites.

4.3 Two compounds show α1β1 preference/selectivity

DCBS199 and DCBS120 show increased efficacy in α1β1 receptors while showing nearly no efficacy at all in α1β3.

DCBS199 shows the best fold ratio of α1β1 preference. It shows no influence by the α1β3 N265S TMD mutation and in addition an identical efficacy in the α1β3 N41R converted receptors hence its efficacy in α1β1 might be generated by the α1β1 ECD interface alone. PQs behaving not only subtype but also binding site selective are highly promising candidates for more specific in vivo effects generated by these compounds compared to benzodiazepines and less selective compounds.

DCBS120 behaves very similar but shows minor influence by the α1β3N265S conversion so it might use the TMD interface in α1β1 receptors to generate some of its efficacy.

When also incorporating data from Simeone et al. (2017) and visible in **Figure 19** the overlapping pharmacophore features of this group of compounds seem to be a hydrogen bond donor at either position R'3 or R'4. In all cases this features come from various types of amino substituents and their related hydrogen atoms.

Again, the R8 substituent on ring D seems to be less of importance. It can again either be a chloro or a methoxy substituent.

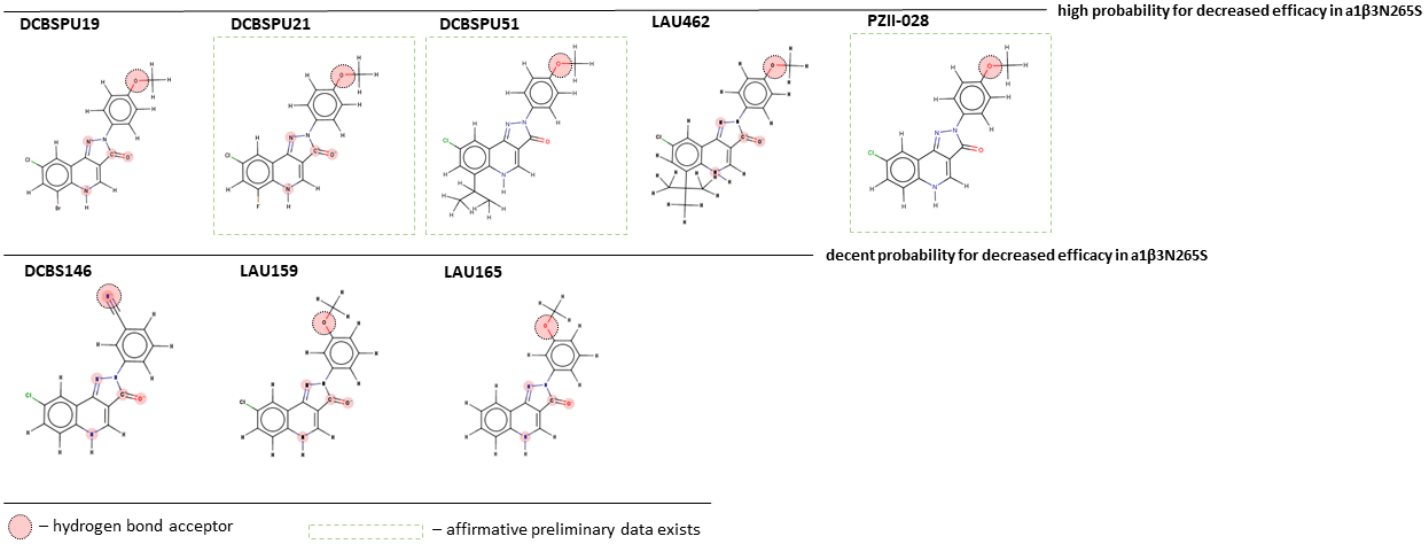

Figure 20 – eight of the most probable virtual screening results which are appearing in all virtual screening approaches involving the TMD interface. Top-row – R'4 substitueted compounds, bottom-row – R'3 substitueted compounds. Also preliminary data and data gathered by other publications are taken into consideration (green borders).

4.4 Virtual screening: predicted PQs with decreased efficacy in α1β3N265S

After the application of all three virtual screening approaches (see results), 10 compounds were appearing in all of them and might have the best chance of being a true positive. **Figure 20** shows 8/10 compounds. As indicated in **Figure 20** all of them have either a R'3 or R'4 hydrogen bond acceptor feature on ring D.

Compounds with a R'4 hydrogen bond acceptor feature substituent might have a higher probability since all compounds in the experimental data that show reduced efficacy in α1β3N265S also have the same feature. For DCBSPU21 preliminary data gives additional affirmation (appendix **Figure 22**). For DCBSPU51 the data is highly variable but also showing trends towards being influenced by the α1β3N265S mutation (**Figure 5**) and for PZII-028 data gathered by Simeone et al. (2017) shows that the α1β3N41R conversion mutation for the ECD α+/β- interface is not fully converting the efficacy to α1β1 so other sites like the TMD β+/α- interface could also play a role and this works variance for PZII-028 might be too high to show these effects.

For compounds with the R'3 hydrogen bond acceptor feature there is no data about TMD binding behaviour available but since all three virtual screening approaches match them there is a chance that they are also using the TMD β+/α- interface in a similar fashion.

In the end it should also be mentioned that PQs can also bind the TMD interface without having an effect, meaning that there might be silent binder as well. Unfortunately, the experimental data one can only identify PQs that show an effect upon binding.

4.5 Substituents on ring D seem to have high influence on effects

Pharmacophore features that seem to influence the effects regarding receptor subtype preference of PQs the most seem to be substituents located on ring D. As visible in **Figure 19** and when grouped by receptor subtype preference the common denominators are always located on ring D on either position R'3 or R'4.

Also, the TMD binding behaviour seems to be influenced by substituents in similar positions.

To summarize, α1β3 preferring compounds have a hydrogen bond acceptor at position R'4, α1β1 preferring compounds have a hydrogen bond donor feature at either position R'3 or R'4 and lastly compounds with no preference have a lipophilic hydrocarbon at position R'4.

4.6 Docking Poses for the TMD Interface predicted with Ligand Scout

Without structural data about ligand-protein interactions, predicting docking poses becomes a game of chances. Nevertheless, scoring functions can have a decent predictive value for correct docking poses which was shown when trying to redock existing ligand-protein complexes (appendix **Figure 21**, **Table 6**). Additionally, considering the population of docking poses can help to identify more probable ones. For example, when docking all PQs used in this work into the TMD interface, docking pose one (**Figure 12**, **appendix Table 7**) is populated with four (DCBSPU53, LAU177, DCBS120, DCBSPU51) out of seven PQs and shows the lowest mean estimated binding energy from all poses. DCBSPU53 and LAU177 are confirmed by experimental data for being TMD binders. DCBSPU51 might as well bind this interface when considering the complete pharmacophore-overlap with DCBSPU53.

The highest populated docking pose from the two best scored poses in regards of estimated binding affinity score is pose 12 (**Figure 12**, **appendix Table 7**). It is appearing for LAU176, LAU177, PZII-028 and DCBS199.

When considering the importance of ring D substitutions on the binding behaviour of PQs, poses where ring D is directed towards the pocket and can interact with amino acids seem to be more likely than poses where ring D sticks out of the pocket. Vice versa the less importance

of ring A substitutions also work along this line of thinking where ring a might have less interactions with the pocket and is located towards the outer side.

4.7 Limitations of the work

In this work only efficacies of compounds at 10 µM were compared which doesn't give the whole picture. To get the whole picture dose response curves and the related EC50 of compounds need to be compared since a shift in EC50 also influences how selective a compound activates a receptor subtype at a certain concentration. Simeone et al. (2017) showed that for some compounds like LAU176, the EC50 in α1β1 is left shifted compared to the EC50 in α1β3 which means that the α1β1 receptor pool gets activated with lower concentrations. Even though the max efficacy at 10 µM is higher in α1β3 this compound is considered potency selective for α1β1 receptors.

Additionally, only a small number of compounds was analysed. To get a better understanding of structure function relationships compounds should have also been systematically varied in regards of their substitutions.

Another limitation of the work is the, in some cases, high variability of datasets. For DCBSPU51 the variability is particularly prominent which makes significant conclusions about this compound hard. The variability of DCBSPU51 might be a result from 10 µM not being peak concentration in terms of maximum efficacy, in other word 10 µM might be still in the rising phase of the dose response which is known to have higher variation than peak efficacy concentrations.

Lastly a big limitation of mutational work is the possibility that a change in amino acids is influencing efficacy in an indirect manner by changing the whole stability and energy dynamics of the protein which means that the whole protein can for example become more rigid if a certain amino acid is changed and thereby affecting the interaction with ligands and conformational changes on a global level. Needless to say, in many cases mutational analysis of binding site is directly related to local interactions with ligands inside the binding site because hypothesis based on mutational work were in many cases confirmed by structural ligand-protein data.

References

Boast, C. A., Snowhill, E. W., & Simke, J. P. (1985). CGS 8216 and CGS 9896, novel pyrazoloquinoline benzodiazepine ligands with benzodiazepine agonist and antagonist properties. *Pharmacology Biochemistry and Behavior*, *23*(4), 639–644. https://doi.org/https://doi.org/10.1016/0091-3057(85)90431-9

Carotti, A., Altomare, C., Savini, L., Chiasserini, L., Pellerano, C., Mascia, M. P., Maciocco, E., Busonero, F., Mameli, M., Biggio, G., & Sanna, E. (2003). High affinity central benzodiazepine receptor ligands. Part 3: insights into the pharmacophore and pattern recognition study of intrinsic activities of pyrazolo[4,3-c]quinolin-3-ones. *Bioorganic & Medicinal Chemistry*, *11*(23), 5259–5272. https://doi.org/https://doi.org/10.1016/S0968-0896(03)00527-3

Fabjan, J., Koniuszewski, F., Schaar, B., & Ernst, M. (2021). Structure-Guided Computational Methods Predict Multiple Distinct Binding Modes for Pyrazoloquinolinones in GABAA Receptors. *Frontiers in Neuroscience*, *14*(January), 1–17. https://doi.org/10.3389/fnins.2020.611953

Griessner, J., Pasieka, M., Böhm, V., Grössl, F., Kaczanowska, J., Pliota, P., Kargl, D., Werner, B., Kaouane, N., Strobelt, S., Kreitz, S., Hess, A., & Haubensak, W. (2021). Central amygdala circuit dynamics underlying the benzodiazepine anxiolytic effect. *Molecular Psychiatry*, *26*(2), 534–544. https://doi.org/10.1038/s41380-018-0310-3

Hill-Venning, C., Belelli, D., Peters, J. A., & Lambert, J. J. (1997). Subunit-dependent interaction of the general anaesthetic etomidate with the gamma-aminobutyric acid type A receptor. *British Journal of Pharmacology*, *120*(5), 749–756. https://doi.org/10.1038/sj.bjp.0700927

Hörtnagl, H., Tasan, R. O., Wieselthaler, A., Kirchmair, E., Sieghart, W., & Sperk, G. (2013). Patterns of mRNA and protein expression for 12 GABAA receptor subunits in the mouse brain. *Neuroscience*, *236*, 345–372. https://doi.org/10.1016/j.neuroscience.2013.01.008

Iorio, M. T., Rehman, S., Bampali, K., Stoeger, B., Schnürch, M., Ernst, M., & Mihovilovic, M. D. (2019). Variations on a scaffold - Novel GABAA receptor

modulators. *European Journal of Medicinal Chemistry*, *180*, 340–349. https://doi.org/10.1016/j.ejmech.2019.07.008

Iorio, M. T., Vogel, F. D., Koniuszewski, F., Scholze, P., Rehman, S., Simeone, X., Schnürch, M., Mihovilovic, M. D., & Ernst, M. (2020). GABAa receptor ligands often interact with binding sites in the transmembrane domain and in the extracellular domain—can the promiscuity code be cracked? *International Journal of Molecular Sciences*, *21*(1). https://doi.org/10.3390/ijms21010334

Johnston, G. A. R. (1996). GABAA receptor pharmacology. *Pharmacology and Therapeutics*, *69*(3), 173–198. https://doi.org/10.1016/0163-7258(95)02043-8

Kim, J. J., Gharpure, A., Teng, J., Zhuang, Y., Howard, R. J., Zhu, S., Noviello, C. M., Jr, R. M. W., Lindahl, E., & Hibbs, R. E. (2020). Shared structural mechanisms of general anaesthetics and benzodiazepines. *Nature*, *585*(September). https://doi.org/10.1038/s41586-020-2654-5

Knutson, D. E., Kodali, R., Divović, B., Treven, M., Stephen, M. R., Zahn, N. M., Dobričić, V., Huber, A. T., Meirelles, M. A., Verma, R. S., Wimmer, L., Witzigmann, C., Arnold, L. A., Chiou, L.-C., Ernst, M., Mihovilovic, M. D., Savić, M. M., Sieghart, W., & Cook, J. M. (2018). Design and Synthesis of Novel Deuterated Ligands Functionally Selective for the γ-Aminobutyric Acid Type A Receptor (GABA(A)R) α6 Subtype with Improved Metabolic Stability and Enhanced Bioavailability. *Journal of Medicinal Chemistry*, *61*(6), 2422–2446. https://doi.org/10.1021/acs.jmedchem.7b01664

Laurie, D. J., Wisden, W., & Seeburg, P. H. (1992). The distribution of thirteen GABA(A) receptor subunit mRNAs in the rat brain. III. Embryonic and postnatal development. *Journal of Neuroscience*, *12*(11), 4151–4172. https://doi.org/10.1523/jneurosci.12-11-04151.1992

Maldifassi, M. C., Baur, R., & Sigel, E. (2016). Molecular mode of action of CGS 9895 at α1β2γ2 GABAA receptors. *Journal of Neurochemistry*, *3*, 722–730. https://doi.org/10.1111/jnc.13711

Masiulis, S., Desai, R., Uchański, T., Martin, I. S., Laverty, D., Karia, D., & Aricescu, A. R. (2019). *GABA A receptor signalling mechanisms revealed by structural*

pharmacology. https://doi.org/10.1038/s41586-018-0832-5

Mohler, H., Martin, L., Mcintosh, H., Julou, L., Fieri, L., & Rinehart, K. (1982). *2-Arylpyrazolo[4,3-c]quinolin-3-ones: Novel Agonist,*. *8*(1981), 337–339.

Nilsson, J., Gidlöf, R., Nielsen, E. Ø., Liljefors, T., Nielsen, M., & Sterner, O. (2011). Triazoloquinazolinediones as novel high affinity ligands for the benzodiazepine site of GABAA receptors. *Bioorganic and Medicinal Chemistry*, *19*(1), 111–121. https://doi.org/10.1016/j.bmc.2010.11.050

Nutt, D. (2006). GABAA receptors: subtypes, regional distribution, and function. *Journal of Clinical Sleep Medicine : JCSM : Official Publication of the American Academy of Sleep Medicine*, *2*(2), S7-11.

Olsen, R. W. (2015). Allosteric ligands and their binding sites define γ-aminobutyric acid (gaba) type a receptor subtypes. In *Advances in Pharmacology* (1st ed., Vol. 73). Elsevier Inc. https://doi.org/10.1016/bs.apha.2014.11.005

Olsen, R. W., & Sieghart, W. (2009). GABA A receptors: subtypes provide diversity of function and pharmacology. *Neuropharmacology*, *56*(1), 141–148. https://doi.org/10.1016/j.neuropharm.2008.07.045

Pirker, S., Schwarzer, C., Wieselthaler, A., Sieghart, W., & Sperk, G. (2000). GABA(A) receptors: immunocytochemical distribution of 13 subunits in the adult rat brain. *Neuroscience*, *101*(4), 815–850. https://doi.org/10.1016/s0306-4522(00)00442-5

Ramerstorfer, J., Furtmüller, R., Sarto-Jackson, I., Varagic, Z., Sieghart, W., & Ernst, M. (2011). The GABAA receptor α+β- interface: A novel target for subtype selective drugs. *Journal of Neuroscience*, *31*(3), 870–877. https://doi.org/10.1523/JNEUROSCI.5012-10.2011

Sanders, M. P. A., Barbosa, A. J. M., Zarzycka, B., Nicolaes, G. A. F., Klomp, J. P. G., de Vlieg, J., & Del Rio, A. (2012). Comparative analysis of pharmacophore screening tools. *Journal of Chemical Information and Modeling*, *52*(6), 1607–1620. https://doi.org/10.1021/ci2005274

Sarto-Jackson, I., & Sieghart, W. (2008). Assembly of GABAA receptors (Review). *Molecular Membrane Biology*, *25*(4), 302–310.

https://doi.org/10.1080/09687680801914516

Shindo, H., Takada, S., Murata, S., Eigyo, M., & Matsushita, A. (1989). Thienylpyrazoloquinolines with high affinity to benzodiazepine receptors: continuous shift from inverse agonist to agonist properties depending on the size of the alkyl substituent. *Journal of Medicinal Chemistry*, *32*(6), 1213–1217. https://doi.org/10.1021/jm00126a012

Sieghart, W., & Savic, M. M. (2018). International union of basic and clinical pharmacology. CVI: GABAA receptor subtype-and function-selective ligands: Key issues in translation to humans. *Pharmacological Reviews*, *70*(4), 836–878. https://doi.org/10.1124/PR.117.014449

Simeone, X., Iorio, M. T., Siebert, D. C. B., Rehman, S., Schnürch, M., Mihovilovic, M. D., & Ernst, M. (2019). Defined concatenated α6α1β3γ2 GABAA receptor constructs reveal dual action of pyrazoloquinolinone allosteric modulators. *Bioorganic and Medicinal Chemistry*, *27*(14), 3167–3178. https://doi.org/10.1016/j.bmc.2019.06.006

Simeone, Xenia, Siebert, D. C. B., Bampali, K., Varagic, Z., Treven, M., Rehman, S., Pyszkowski, J., Holzinger, R., Steudle, F., Scholze, P., Mihovilovic, M. D., Schnürch, M., & Ernst, M. (2017). Molecular tools for GABAA receptors: High affinity ligands for β1-containing subtypes. *Scientific Reports*, *7*(1), 1–12. https://doi.org/10.1038/s41598-017-05757-4

Stewart, D. S., Pierce, D. W., Hotta, M., Stern, A. T., & Forman, S. A. (2014). Mutations at Beta N265 in γ-Aminobutyric Acid Type A Receptors Alter Both Binding Affinity and Efficacy of Potent Anesthetics. *PLOS ONE*, *9*(10), e111470. https://doi.org/10.1371/journal.pone.0111470

Treven, M., Siebert, D. C. B., Holzinger, R., Bampali, K., Fabjan, J., Varagic, Z., Wimmer, L., Steudle, F., Scholze, P., Schnürch, M., Mihovilovic, M. D., & Ernst, M. (2018). Towards functional selectivity for α6β3γ2 GABAA receptors: a series of novel pyrazoloquinolinones. *British Journal of Pharmacology*, *175*(3), 419–428. https://doi.org/10.1111/bph.14087

Varagic, Z., Wimmer, L., Schnürch, M., Mihovilovic, M. D., Huang, S., Rallapalli, S., Cook,

J. M., Mirheydari, P., Ecker, G. F., Sieghart, W., & Ernst, M. (2013). Identification of novel positive allosteric modulators and null modulators at the GABAA receptor α+β- interface. *British Journal of Pharmacology*, *169*(2), 371–383. https://doi.org/10.1111/bph.12151

Vega Alanis, B. A., Iorio, M. T., Silva, L. L., Bampali, K., Ernst, M., Schnürch, M., & Mihovilovic, M. D. (2020). Allosteric GABAA Receptor Modulators—A Review on the Most Recent Heterocyclic Chemotypes and Their Synthetic Accessibility. *Molecules*, *25*(4). https://doi.org/10.3390/molecules25040999

Wolber, G., & Langer, T. (2005). LigandScout: 3-D pharmacophores derived from protein-bound ligands and their use as virtual screening filters. *Journal of Chemical Information and Modeling*, *45*(1), 160–169. https://doi.org/10.1021/ci049885e

Wongsamitkul, N., Maldifassi, M. C., Simeone, X., Baur, R., Ernst, M., & Sigel, E. (2017). α subunits in GABAA receptors are dispensable for GABA and diazepam action. *Scientific Reports*, *7*(1), 1–11. https://doi.org/10.1038/s41598-017-15628-7

Appendix

4.8 Appendix

Table 5 – Database of various PQs used for the virtual screenings.

Compounds	R8	R7	R6	R4'	R3'
DCBS192	Cl	H	H	Br	H
LAU161	Cl	H	H	CN	H
DCBSLK36	Cl	H	H	CO-NH2	H
DCBS128_D	Cl	H	H	COO-	H
LAU162	Cl	H	H	COOEt	H
DCBS128	Cl	H	H	COOH	H
DCBS32	Cl	H	H	H	Br
DCBS146	Cl	H	H	H	CN
DCBS152B	Cl	H	H	H	CO-NH2
DCBS152A_D	Cl	H	H	H	COO-
DCBS152A	Cl	H	H	H	COOH
LAU163	Cl	H	H	H	H
DCBS142	Cl	H	H	H	Me
DCBS120	Cl	H	H	H	NH2
DCBS119	Cl	H	H	H	NO2
DCBSPU19	Cl	H	Br	H	OMe
LAU159	Cl	H	H	H	OMe
LAU156	Cl	H	H	Me	H
LAU206	Cl	H	H	NH2	H
LAU157	Cl	H	H	NO2	H
DCBSPU21	Cl	H	F	OMe	H
DCBSPU26	Cl	H	Me	OMe	H
DCBSPU27	Cl	H	Cl	OMe	H
DCBSPU51	Cl	H	iPr	OMe	H
DCBSPU53	Cl	H	Et	OMe	H
LAU462	Cl	H	tbut	OMe	H
PZII028	Cl	H	H	OMe	H
XHEII087C	H	H	tbut	Br	H
XHEIII006C	H	Br	H	Br	H
XHEIIII063	H	H	H	C≡CH	H
CGS9896	H	H	H	Cl	H
CGS8216	H	H	H	H	H
PWZ009A1	H	OMe	H	H	H
LAU165	H	H	H	H	OMe
CGS9895	H	H	H	OMe	H
PZII029	H	OMe	H	OMe	H
PBXHE	Me	Me	H	Br	H
LAU177	OMe	H	H	CN	H
DCBSLK60	OMe	H	H	CO-NH2	H

DCBS145	OMe	H	H	H	CN
DCBS151B	OMe	H	H	H	CO-NH2
DCBS88_D	OMe	H	H	H	COO-
DCBS151A_D	OMe	H	H	H	COO-
DCBS88	OMe	H	H	H	COOH
DCBS151A	OMe	H	H	H	COOH
PWZ007A	OMe	H	H	H	H
DCBS76	OMe	H	H	Me	H
DCBS141	OMe	H	H	H	Me
DCBSLS24	OMe	H	H	H	NH2
DCBS52	OMe	H	H	H	NO2
DCBS135	OMe	H	H	H	OMe
DCBS96	OMe	H	H	NH2	H
DCBS93	OMe	H	H	NO2	H
LAU176	OMe	H	H	OMe	H
XHEII006	tbut	H	H	Br	H
XHEII17	tbut	H	H	C≡CH	H
XHEIII24	tbut	H	H	F	H

Table 6 – Validation results – redocking of pubslished ligand-protein complexes, marked in green are correctly redocked poses

Ligand	Binding Energy (kcal/mol)	Binding Affinity Score
(6HUP) [D] DZP2001 [1]	-7.8	-23.7
(6HUP) [D] DZP2001 [2]	-7.79	-25.18
(6HUP) [D] DZP2001 [3]	-7.69	-18.44
(6HUO) [D] 08H501 [1]	-9.63	-30.16
(6HUO) [D] 08H501 [2]	-8.8	-17.67
(6X3V) [A] V8D406 [1]	-6.5	-20.56
(6X3V) [A] V8D406 [2]	-6.45	-21.32
(6X3V) [A] V8D406 [3]	-6.06	-19.4
(6X3V) [A] V8D406 [4]	-5.78	-17.01
(6X3V) [A] V8D406 [5]	-5.77	-17.56
(6X3V) [A] V8D406 [6]	-5.76	-17.03

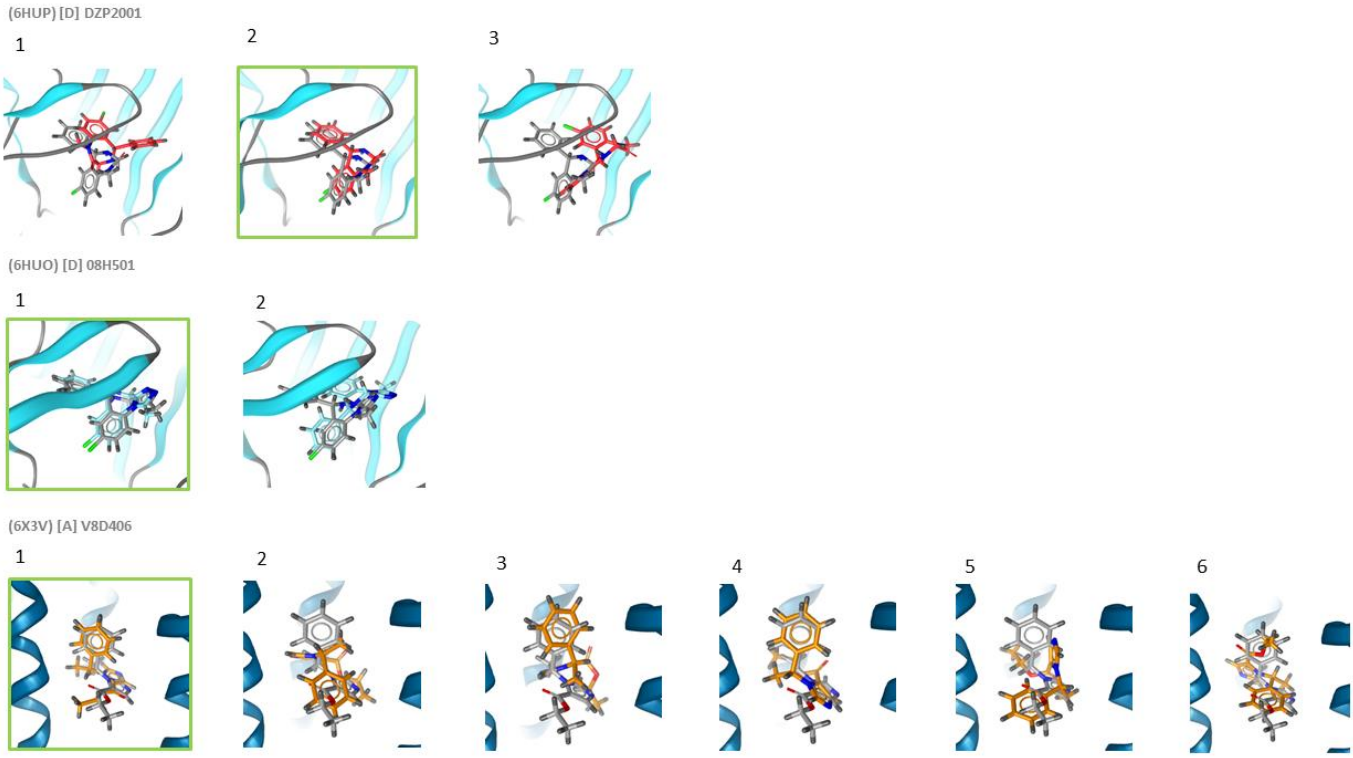

Figure 21 – docking poses of redocked ligands done for validation. The numbers above the pictures indicates the pose number (e.g "(6HUP) [D] DZP2001 [1]" from **Table 5** corresponds to the pose in the top row with the number 1). Green borders indicate correctly redocked poses.

Table 7 – Docking results performed with AutoDock4 in LigandScout for all PQs used in this work, PDB structure: 6X3V [A] V8D406. Green rows: poses with best Binding Energy (kcal/mol), blue rows: poses with best Binding Affinity Score.

Ligand	Binding Energy (kcal/mol)	Binding Affinity Score	bindingmode
DCBSPU51 [1]	-8.21	-27.12	1
DCBSPU51 [2]	-7.33	-24.78	2
DCBSPU51 [3]	-6.9	-28.76	3
DCBSPU51 [4]	-6.71	-28.52	4
DCBSPU51 [5]	-6.6	-31.11	5
DCBSPU51 [6]	-6.46	-28.74	6
DCBS120 [1]	-7.71	-18.01	1
DCBS120 [2]	-7.44	-24.15	3
DCBS120 [3]	-7.38	-28.17	8
DCBS120 [4]	-7.18	-21.88	6
DCBSPU53 [1]	-7.94	-23.85	1
DCBSPU53 [2]	-7.53	-25.43	9
DCBSPU53 [3]	-7.03	-25.43	4
DCBSPU53 [4]	-7	-28.48	3
DCBSPU53 [5]	-6.7	-25.32	10

DCBSPU53 [6]	-6.38	-28.7	6
DCBSPU53 [7]	-6.32	-29.22	5
LAU176 [1]	-6.97	-22.15	11
LAU176 [2]	-6.94	-25.64	12
LAU176 [3]	-6.66	-22.16	0
LAU176 [4]	-6.62	-19.13	0
LAU177 [1]	-7.47	-18.49	1
LAU177 [2]	-7.47	-24.45	12
LAU177 [3]	-7.05	-18.84	11
PZII028 [1]	-7.44	-26.2	0
PZII028 [2]	-7.24	-32.65	12
PZII028 [3]	-6.85	-27.98	11
DCBS199 [1]	-7.85	-19.6	8
DCBS199 [2]	-7.58	-24.65	17
DCBS199 [3]	-7.08	-21.13	15
DCBS199 [4]	-7.07	-22.86	10
DCBS199 [5]	-6.77	-22.03	16

Table 8 – Screening results of approach 3. Two docking-pose-derived-pharmacophores-screenings per PQ were performed.

Ligand	Pharmacophore Fit Score	From
LAU462	47.67	DCBSPU53 [1]
DCBSPU26	47.51	DCBSPU53 [1]
DCBSPU51	47.33	DCBSPU53 [1]
PZII028	47.12	DCBSPU53 [1]
DCBSPU53	47.09	DCBSPU53 [1]
DCBSPU51	48.39	DCBSPU53 [7]
DCBSPU53	48.02	DCBSPU53 [7]
DCBS145	48.31	LAU176 [1]
DCBSLS24	47.23	LAU176 [1]
DCBS52	47.23	LAU176 [1]
DCBS151A	47.22	LAU176 [1]
PWZ007A	45.73	LAU176 [1]
DCBS141	45.7	LAU176 [1]
LAU161	38.97	LAU177 [1]
LAU177	38.97	LAU177 [1]
DCBSPU27	38.64	LAU177 [2]
DCBSPU21	38.64	LAU177 [2]
DCBSPU19	38.61	LAU177 [2]
LAU159	38.5	LAU177 [2]
DCBS135	38.5	LAU177 [2]
DCBS146	38.45	LAU177 [2]

XHEIII006C	37.93	LAU177 [2]
PZII029	37.93	LAU177 [2]
XHEIII063	37.85	LAU177 [2]
LAU165	37.85	LAU177 [2]
CGS8216	37.85	LAU177 [2]
DCBS151B	37.53	LAU177 [2]
DCBSLS24	37.38	LAU177 [2]
DCBS152A	37.33	LAU177 [2]
DCBS151A	37.32	LAU177 [2]
PBXHE	37.05	LAU177 [2]

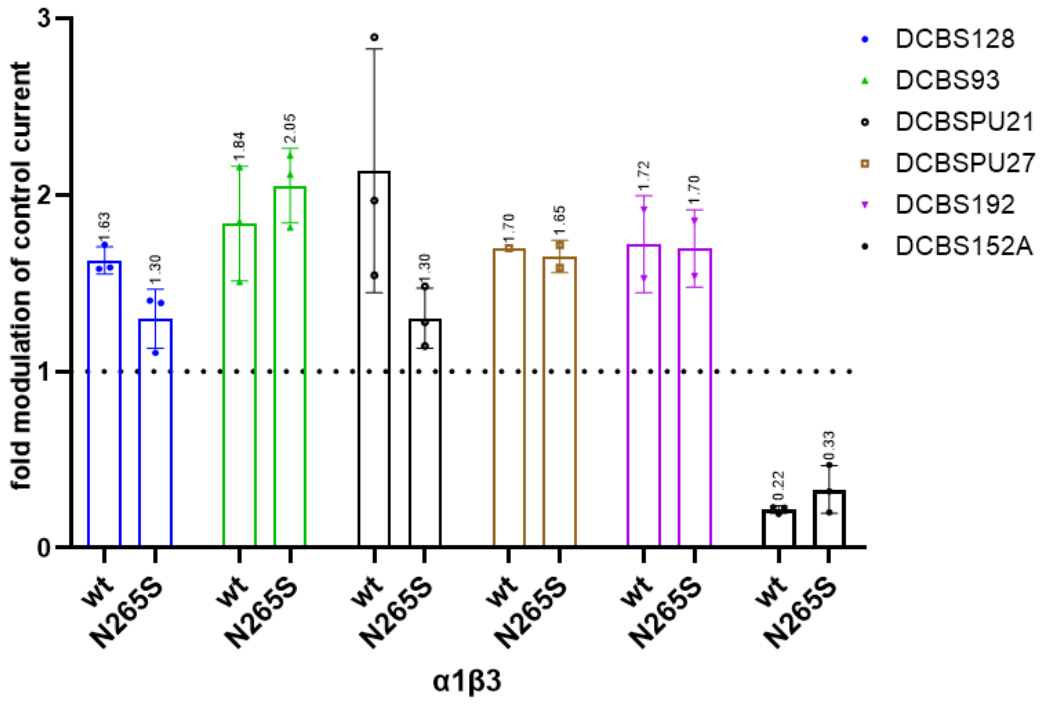

Figure 22 – Preliminary data for DCBS120, DCBS93, DCBSPU21, DCBSPU27, DCBS192, DCBS152A in α1β3wt and α1β3N265S receptors. Fold modulation of control current - mean with sd, n = 3.

4.9 Zusammenfassung (Abstract - Deutsch)

Pyrazolochinolinone (PQs) sind vielversprechende Substanzen für $GABA_A$-Rezeptorsubtypen-selektive Arzneimittel. Es ist bereits bekannt, dass PQs eine neu Bindestelle in der extrazellulären Domain (EZD α+/β- Interface) binden können und über diese positive allosterische Modulation erzeugen. Bis jetzt wurde noch keine Substanz identifiziert welche ausschließlich diese neue Bindestelle verwendet. Substanzen, welche diese Bindestelle verwenden, könnten andere Rezeptor Populationen aktivieren als Substanzen, welche an die kanonische Benzodiazepin-Bindestelle binden und daher ein anderes Wirkungs- und Nebenwirkungs- Spektrum erwartet wird. Es wurde gezeigt, dass einige PQs auch an einer Bindestelle in der Transmembrandomäne (TMD β+/α- Interface) binden können, jedoch fehlt es an Daten bezüglich der Involvierung dieser Bindestelle für viele PQ-Derivate. Beteiligung der TMD an der Wirkung führt zu einem Verlust von Selektivität da die TMD konservierter ist als die ECD. Darum ist es notwendig mehr Daten bezüglich des Bindungsverhaltens verschiedenster PQ-Derivate zu sammeln, um besser einschätzen zu können welche Chemischen Eigenschaften das Binden/Nicht-Binden and die TMD Bindestelle begünstigen. In dieser Arbeit wurde die Wirksamkeit von sieben PQ-Derivaten (PZII-028, DCBS120, DCBS199, DCBSPU51, DCBSPU53, LAU176, LAU177) durch Zwei-Elektroden-Voltage-Clamp in α1β3, α1β3N265S, α1β3N41R and α1β1 Rezeptoren analysiert. Während viele der Derivate (LAU176, LAU177, DCBSPU53, DCBS120) an der TMD Bindestelle (TMD β+/α-Interface) binden, zeigt ein Derivat (DCBS199) Selektivität für das EZD α+/β- Interface in α1β1 Rezeptoren, ohne an der TMD Bindestelle zu binden. Das Binden an die TMD Bindestelle in α1β3 Rezeptoren scheint durch einen Wasserstoffbrückenakzeptor an Position R‘4 begünstigt zu werden. Zusätzlich zeigen Derivate mit diesem Merkmal auch höhere Wirksamkeit in α1β3 Rezeptoren. Ein Derivat (DCBS120) scheint die TMD Bindestelle in α1β1 Rezeptoren zu verwenden. Dieses Derivat hat einen Wasserstoffbrückendonor and Position R‘3. Zwei Derivate (DCBS120, DCBS199) zeigen höhere Wirksamkeit in α1β1 Rezeptoren und beide haben einen Amino-Substituenten an Ring D entweder in Position R‘3 (DCBS120) oder R‘4 (DCBS199). Das Binden and die TMD bindestelle scheint stark von Substituenten auf Ring D beeinflusst zu werden und weniger stark von Ring A Substitutionen. Zu guter Letzt wurde ein virtuelles Screening einer Datenbank von 57 weiteren PQ Derivaten mit Ligand Scout durchgeführt. Auch diese Methode prognostiziert Binding an der TMD für etliche Derivate.

4.10 Acknowledgements

Lastly, I want to thank my supervisor Margot and the whole team for guiding me through this last step of my master's degree. I am especially thankful for the enjoyable working atmosphere in the team, and it was a pleasure working with you all!

I also want to thank my family for the support and the possibility to chase my interests and dreams and for the trust in my decisions, wherever they will lead.